

OPEN

Optimizing High-Efficiency Quantum Memory with Quantum Machine Learning for Near-Term Quantum Devices

Laszlo Gyongyosi^{1,2,3*} & Sandor Imre²

Quantum memories are a fundamental of any global-scale quantum Internet, high-performance quantum networking and near-term quantum computers. A main problem of quantum memories is the low retrieval efficiency of the quantum systems from the quantum registers of the quantum memory. Here, we define a novel quantum memory called high-retrieval-efficiency (HRE) quantum memory for near-term quantum devices. An HRE quantum memory unit integrates local unitary operations on its hardware level for the optimization of the readout procedure and utilizes the advanced techniques of quantum machine learning. We define the integrated unitary operations of an HRE quantum memory, prove the learning procedure, and evaluate the achievable output signal-to-noise ratio values. We prove that the local unitaries of an HRE quantum memory achieve the optimization of the readout procedure in an unsupervised manner without the use of any labeled data or training sequences. We show that the readout procedure of an HRE quantum memory is realized in a completely blind manner without any information about the input quantum system or about the unknown quantum operation of the quantum register. We evaluate the retrieval efficiency of an HRE quantum memory and the output SNR (signal-to-noise ratio). The results are particularly convenient for gate-model quantum computers and the near-term quantum devices of the quantum Internet.

Quantum memories are a fundamental of any global-scale quantum Internet^{1–6}. However, while quantum repeaters can be realized without the necessity of quantum memories^{1,3}, these units, in fact, are required for guaranteeing an optimal performance in any high-performance quantum networking scenario^{3,4,7–32}. Therefore, the utilization of quantum memories still represents a fundamental problem in the quantum Internet^{33–42}, since the near-term quantum devices (such as quantum repeaters^{5,6,8,32,43–47}) and gate-model quantum computers^{48–59} have to store the quantum states in their local quantum memories^{43–47,60–84}. The main problem here is the efficient readout of the stored quantum systems and the low retrieval efficiency of these systems from the quantum registers of the quantum memory. Currently, no general solution to this problem is available, since the quantum register evolves the stored quantum systems via an unknown operation, and the input quantum system is also unknown, in a general scenario^{4,5,7–9,11,12}. The optimization of the readout procedure is therefore a hard and complex problem. Several physical implementations have been developed in the last few years^{85–105}. However, these experimental realizations have several drawbacks, in general because the output signal-to-noise ratio (SNR) values are still not satisfactory for the construction of a powerful, global-scale quantum communication network. As another important application field in quantum communication, the methods of quantum secure direct communication^{106–109} also require quantum memory.

Here, we define a novel quantum memory called high-retrieval-efficiency (HRE) quantum memory for near-term quantum devices. An HRE quantum memory unit integrates local unitary operations on its hardware level for the optimization of the readout procedure. An HRE quantum memory unit utilizes the advanced techniques of quantum machine learning to achieve a significant improvement in the retrieval efficiency^{110–112}. We define the integrated unitary operations of an HRE quantum memory, prove the learning procedure, and evaluate

¹School of Electronics and Computer Science, University of Southampton, Southampton, SO17 1BJ, UK.

²Department of Networked Systems and Services, Budapest University of Technology and Economics, Budapest, H-1117, Hungary. ³MTA-BME Information Systems Research Group, Hungarian Academy of Sciences, Budapest, H-1051, Hungary. *email: l.gyongyosi@soton.ac.uk

the achievable output SNR values. The local unitaries of an HRE quantum memory achieve the optimization of the readout procedure in an unsupervised manner without the use of any labeled data or any training sequences. The readout procedure of an HRE quantum memory is realized in a completely blind manner. It requires no information about the input quantum system or about the quantum operation of the quantum register. (It is motivated by the fact that this information is not accessible in any practical setting).

The proposed model assumes that the main challenge is the recovery of the stored quantum systems from the quantum register of the quantum memory unit, such that both the input quantum system and the transformation of the quantum memory are unknown. The optimization problem of the readout process also integrates the efficiency of the write-in procedure. In the proposed model, the noise and uncertainty added by the write-in procedure are included in the unknown transformation of the QR quantum register of the quantum memory that results in a σ_{QR} mixed quantum system in QR.

The novel contributions of our manuscript are as follows:

1. We define a novel quantum memory called high-retrieval-efficiency (HRE) quantum memory.
2. An HRE quantum memory unit integrates local unitary operations on its hardware level for the optimization of the readout procedure and utilizes the advanced techniques of quantum machine learning.
3. We define the integrated unitary operations of an HRE quantum memory, prove the learning procedure, and evaluate the achievable output signal-to-noise ratio values. We prove that local unitaries of an HRE quantum memory achieve the optimization of the readout procedure in an unsupervised manner without the use of any labeled data or training sequences.
4. We evaluate the retrieval efficiency of an HRE quantum memory and the output SNR.
5. The proposed results are convenient for gate-model quantum computers and near-term quantum devices.

This paper is organized as follows. Section 2 defines the system model and the problem statement. Section 3 evaluates the integrated local unitary operations of an HRE quantum memory. Section 4 proposes the retrieval efficiency in terms of the achievable output SNR values. Finally, Section 5 concludes the results. Supplemental material is included in the Appendix.

System Model and Problem Statement

System model. Let ρ_{in} be an unknown input quantum system formulated by n unknown density matrices,

$$\rho_{in} = \sum_{i=1}^n \lambda_i^{(in)} |\psi_i\rangle \langle \psi_i|, \quad (1)$$

where $\lambda_i^{(in)} \geq 0$, and $\sum_{i=1}^n \lambda_i^{(in)} = 1$.

The input system is received and stored in the QR quantum register of the HRE quantum memory unit. The quantum systems are d -dimensional systems ($d = 2$ for a qubit system). For simplicity, we focus on $d = 2$ dimensional quantum systems throughout the derivations.

The U_{QR} unknown evolution operator of the QR quantum register defines a mixed state σ_{QR} as

$$\begin{aligned} \sigma_{QR} &= U_{QR} \rho_{in} U_{QR}^\dagger \\ &= \sum_{i=1}^n \lambda_i |\phi_i\rangle \langle \phi_i|, \end{aligned} \quad (2)$$

where $\lambda_i \geq 0$, $\sum_{i=1}^n \lambda_i = 1$.

Let us allow to rewrite (2) for a particular time t , $t = 1, \dots, T$, where T is a total evolution time, via a mixed system $\sigma_{QR}^{(t)}$, as

$$\begin{aligned} \sigma_{QR}^{(t)} &= U_{QG}^{(t)} \rho_{in} \left(U_{QG}^{(t)} \right)^\dagger \\ &= \sum_{i=1}^n \lambda_i^{(t)} |\phi_i^{(t)}\rangle \langle \phi_i^{(t)}| \\ &= \sum_{i=1}^n \left(\sqrt{\lambda_i^{(t)}} |\phi_i^{(t)}\rangle \right) \left(\sqrt{\lambda_i^{(t)}} \langle \phi_i^{(t)}| \right) \\ &= \sum_{i=1}^n X_i^{(t)} \left(X_i^{(t)} \right)^\dagger \\ &= X^{(t)} \left(X^{(t)} \right)^\dagger, \end{aligned} \quad (3)$$

where $U_{QR}^{(t)}$ is an unknown evolution matrix of the QR quantum register at a given t , with a dimension

$$\dim \left(U_{QR}^{(t)} \right) = d^n \times d^n, \quad (4)$$

with $0 \leq \lambda_i^{(t)} \leq 1$, $\sum_i \lambda_i^{(t)} = 1$, while $X_i^{(t)} \in \mathbb{C}$ is an unknown complex quantity, defined as

$$X_i^{(t)} = \sqrt{\lambda_i^{(t)}} |\phi_i^{(t)}\rangle \quad (5)$$

and

$$X^{(t)} = \sum_{i=1}^n X_i^{(t)}. \quad (6)$$

Then, let us rewrite $\sigma_{QR}^{(t)}$ from (3) as

$$\sigma_{QR}^{(t)} = \rho_{in} + \zeta_{QR}^{(t)} \quad (7)$$

where ρ_{in} is as in (1), and $\zeta_{QR}^{(t)}$ is an unknown residual density matrix at a given t .

Therefore, (7) can be expressed as a sum of M source quantum systems,

$$\sigma_{QR}^{(t)} = \sum_{m=1}^M \rho_m, \quad (8)$$

where ρ_m is the m -th source quantum system and $m = 1, \dots, M$, where

$$M = 2, \quad (9)$$

in our setting, since

$$\rho_1 = \rho_{in} \quad (10)$$

and

$$\rho_2 = \zeta_{QR}^{(t)}. \quad (11)$$

In terms of the M subsystems, (3) can be rewritten as

$$\begin{aligned} \sigma_{QR}^{(t)} &= \sum_{m=1}^M \sum_{i=1}^n \lambda_i^{(m,t)} |\phi_i^{(m,t)}\rangle \langle \phi_i^{(m,t)}| \\ &= \sum_{m=1}^M \sum_{i=1}^n \sqrt{\lambda_i^{(m,t)}} |\phi_i^{(m,t)}\rangle \sqrt{\lambda_i^{(m,t)}} \langle \phi_i^{(m,t)}| \\ &= \sum_{m=1}^M \sum_{i=1}^n X_i^{(m,t)} (X_i^{(m,t)})^\dagger \\ &= \sum_{m=1}^M X^{(m,t)} (X^{(m,t)})^\dagger, \end{aligned} \quad (12)$$

where $X_i^{(m,t)}$ is a complex quantity associated with an m -th source system,

$$X_i^{(m,t)} = \sqrt{\lambda_i^{(m,t)}} |\phi_i^{(m,t)}\rangle, \quad (13)$$

with $0 \leq \lambda_i^{(m,t)} \leq 1$, $\sum_m \sum_i \lambda_i^{(m,t)} = 1$, and

$$X^{(m,t)} = \sum_{i=1}^n X_i^{(m,t)}. \quad (14)$$

The aim is to find the V_{QG} inverse matrix of the unknown evolution matrix U_{QR} in (2), as

$$V_{QG} = U_{QG}^{-1} \quad (15)$$

that yields the separated readout quantum system of the HRE quantum memory unit for $t = 1, \dots, T$, such that for a given t ,

$$\sigma_{out}^{(t)} = V_{QG}^{(t)} \sigma_{QR}^{(t)} (V_{QG}^{(t)})^\dagger, \quad (16)$$

where

$$V_{QG}^{(t)} = (U_{QG}^{(t)})^{-1}. \quad (17)$$

For a total evolution time T , the target σ_{out} density matrix is yielded at the output of the HRE quantum memory unit, as

$$\sigma_{out} \approx \sum_{i=1}^n \lambda_i^{(in)} |\psi_i\rangle \langle \psi_i| \quad (18)$$

with a sufficiently high SNR value,

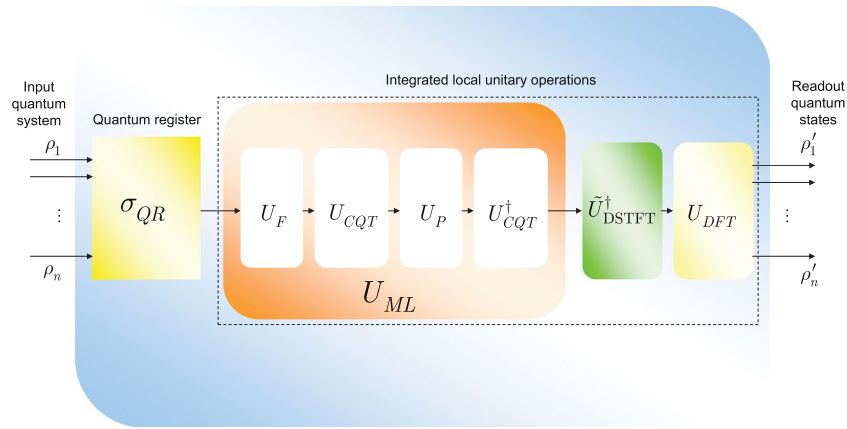


Figure 1. The schematic model of a high-retrieval-efficiency (HRE) quantum memory unit. The HRE quantum memory unit contains a QR quantum register and integrated local unitary operations. The n input quantum systems, $\rho_1 \dots \rho_n$, are received and stored in the quantum register. The state of the QR quantum register defines a mixed state, $\sigma_{QR} = \sum_i \lambda_i \rho_i$, where $\sum_i \lambda_i = 1$. The stored density matrices of the QR quantum register are first transformed by a U_{ML} , a quantum machine learning unitary (depicted by the orange-shaded box) that implements an unsupervised learning for a blind separation of the unlabeled input, and decomposable as $U_{ML} = U_F U_{CQT} U_P U_{CQT}^\dagger$, where U_F is a factorization unitary, U_{CQT} is the quantum constant Q transform with a windowing function f_W for the localization of the wave functions of the quantum register, U_P is a basis partitioning unitary, while U_{CQT}^\dagger is the inverse of U_{CQT} . The result of U_{ML} is processed further by the $\tilde{U}_{DSTFT}^\dagger$ unitary (depicted by the green-shaded box) that realizes the inverse quantum discrete short-time Fourier transform (DSTFT) operation (depicted by the yellow-shaded box), and by the U_{DFT} (quantum discrete Fourier transform) unitary to yield the desired output $\rho'_1 \dots \rho'_n$.

$$\text{SNR}(\sigma_{out}) \geq x, \quad (19)$$

where x is an SNR value that depends on the actual physical layer attributes of the experimental implementation.

The problem is therefore that both the input quantum system (1) and the transformation matrix U_{QR} in (2) of the quantum register are unknown. As we prove, by integrating local unitaries to the HRE quantum memory unit, the unknown evolution matrix of the quantum register can be inverted, which allows us to retrieve the quantum systems of the quantum register. The retrieval efficiency will be also defined in a rigorous manner.

Problem statement. The problem statement is as follows.

Let M be the number of source systems in the QR quantum register such that the sum of the M source systems identifies the mixed state of the quantum register. Let m be the index of the source system, $m = 1, \dots, M$, such that $m = 1$ identifies the unknown input quantum system stored in the quantum register (target source system), while $m = 2, \dots, M$ are some unknown residual quantum systems. The input quantum system, the residual systems, and the transformation operation of the quantum register are unknown. The aim is then to define local unitary operations to be integrated on the HRE quantum memory unit for an HRE readout procedure in an unsupervised manner with unlabeled data.

The problems to be solved are summarized in Problems 1–4.

Problem 1. Find an unsupervised quantum machine learning method, U_{ML} , for the factorization of the unknown mixed quantum system of the quantum register via a blind separation of the unlabeled quantum register. Decompose the unknown mixed system state into a basis unitary and a residual quantum system.

Problem 2. Define a unitary operation for partitioning the bases with respect to the source systems of the quantum register.

Problem 3. Define a unitary operation for the recovery of the target source system.

Problem 4. Evaluate the retrieval efficiency of the HRE quantum memory in terms of the achievable SNR.

The resolutions of the problems are proposed in Theorems 1–4.

The schematic model of an HRE quantum memory unit is depicted in Fig. 1.

The procedures realized by the integrated unitary operations of the HRE quantum memory are depicted in Fig. 2.

Experimental implementation. An experimental implementation of an HRE quantum memory in a near-term quantum device⁵² can integrate standard photonics devices, optical cavities and other fundamental physical devices. The quantum operations can be realized via the framework of gate-model quantum

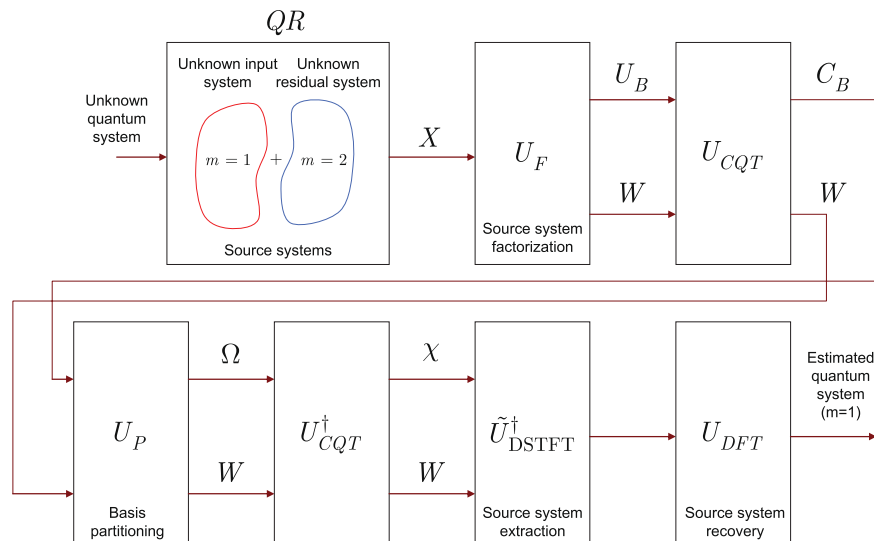


Figure 2. Detailed procedures of an HRE quantum memory. The unknown input quantum system is stored in the QR quantum register that realizes an unknown transformation. The density matrix of the quantum register is the sum of $M = 2$ source systems, where source system $m = 1$ identifies the valuable unknown input quantum system stored in the quantum register, while $m = 2$ identifies an unknown undesired residual quantum system. The U_F unitary evaluates K bases for the source system and defines a W auxiliary quantum system. The U_{CQT} unitary is a preliminary operation for the partitioning of the K bases onto M clusters via unitary U_P . The U_P unitary regroups the bases with respect to the $M = 2$ source systems. The results are then processed by the $\tilde{U}_{DSTFT}^\dagger$ and U_{DFT} unitaries to extract the source system $m = 1$ on the output of the memory unit.

computations of near-term quantum devices^{52–56}, such as superconducting units⁵³. The application of a HRE quantum memory in a quantum Internet setting^{1,2,4–6} can be implemented via noisy quantum links between the quantum repeaters^{8,32,43–47} (e.g., optical fibers^{7,62,113}, wireless quantum channels^{27,28}, free-space optical channels¹¹⁴) and fundamental quantum transmission protocols^{24,115–117}.

Integrated Local Unitaries

This section defines the local unitary operations integrated on an HRE quantum memory unit.

Quantum machine learning unitary. The U_{ML} quantum machine learning unitary implements an unsupervised learning for a blind separation of the unlabeled quantum register. The U_{ML} unitary is defined as

$$U_{ML} = U_F U_{CQT} U_P U_{CQT}^\dagger, \tag{20}$$

where U_F is a factorization unitary, U_{CQT} is the quantum constant Q transform, U_P is a partitioning unitary, while U_{CQT}^\dagger is the inverse of U_{CQT} . **Theorem 1.** (Factorization of the unknown mixed quantum system of the quantum register). The U_F unitary factorizes the unknown σ_{QR} mixed quantum system of the QR quantum register into a unitary $u_{mk} = e^{-iH_{mk}\tau/\hbar}$, with a Hamiltonian H_{mk} and application time τ , and into a system w_{kt} , where $t = 1, \dots, T$, $m = 1, \dots, M$, and $k = 1, \dots, K$, and where T is the evolution time, M is the number of source systems of σ_{QR} , and K is the number of bases.

Proof. The aim of the U_F factorization unitary is to factorize the mixed quantum register (2) into a basis matrix U_B and a quantum system $\vec{\rho}_W$, as

$$\begin{aligned} U_F \vec{\sigma}_{QR} U_F^\dagger &= U_F (U_{QR} \rho_{in} U_{QR}^\dagger) U_F^\dagger \\ &= U_B \vec{\rho}_W U_B^\dagger, \end{aligned} \tag{21}$$

where U_B is a complex basis matrix, defined as

$$U_B = \{u_{mk}\} \in \mathbb{C}^{M \times K}, \tag{22}$$

and $\vec{\rho}_W \in \mathbb{C}^{K \times T}$ is a complex matrix, defined as

$$\vec{\rho}_W = \{\rho_W^{(t)}\}_{t=1}^T, \tag{23}$$

where

$$\begin{aligned}\rho_W^{(t)} &= \sum_{k=1}^K v_k^{(t)} |\varphi_k\rangle \langle \varphi_k| \\ &= \sum_{k=1}^K \sqrt{v_k^{(t)}} |\varphi_k\rangle \sqrt{v_k^{(t)}} \langle \varphi_k| \\ &= \sum_{k=1}^K W_k^{(t)} (W_k^{(t)})^\dagger,\end{aligned}\quad (24)$$

where $0 \leq v_k^{(t)} \leq 1$, and $\sum_{k=1}^K v_k^{(t)} = 1$, while K is the total number of bases of U_B , while $W_k^{(t)} \in \mathbb{C}$ is a complex quantity, as

$$W_k^{(t)} = \sqrt{v_k^{(t)}} |\varphi_k\rangle. \quad (25)$$

The first part of the problem is therefore to find (22), where u_{mk} is a unitary that sets a computational basis for $W_k^{(t)}$ in (25), defined as

$$u_{mk} = e^{-iH_{mk}\tau/\hbar}, \quad (26)$$

where H_{mk} is a Hamiltonian, as

$$H_{mk} = G_{mk} |k_m\rangle \langle k_m|, \quad (27)$$

where G_{mk} is the eigenvalue of basis $|k_m\rangle$, $H_{mk} |k_m\rangle = G_{mk} |k_m\rangle$, while τ is the application time of u_{mk} .

The second part of the problem is to determine W , as

$$W = \{W_k^{(t)} = w_{kt}\} \in \mathbb{C}^{K \times T}, \quad (28)$$

where $W_k^{(t)} = w_{kt}$ is a system state, that formulates $\tilde{X}^{(m,t)}$ as

$$\begin{aligned}\tilde{X}^{(m,t)} &= [U_B W]_{mt} \\ &= \sum_{k=1}^K u_{mk} w_{kt},\end{aligned}\quad (29)$$

where $\tilde{X}^{(m,t)}$ is an approximation of $X^{(m,t)}$,

$$\tilde{X}^{(m,t)} \approx X^{(m,t)}, \quad (30)$$

where $X^{(m,t)}$ is defined in (14).

As follows, for the total evolution time T , $\vec{X} \in \mathbb{C}^{M \times T}$ can be defined as

$$\vec{X} = \{X^{(1,t)}, \dots, X^{(M,t)}\}_{t=1}^T, \quad (31)$$

and the challenge is to evaluate (31) as a decomposition

$$\begin{aligned}\tilde{X} &= U_B W \\ &= e^{-iH_S \tau/\hbar} W \\ &= \sum_{m=1}^M \sum_{t=1}^T \sum_{k=1}^K u_{mk} W_k^{(t)} \\ &= \sum_{m=1}^M \sum_{t=1}^T \sum_{k=1}^K e^{-iH_{mk}\tau/\hbar} \sqrt{v_k^{(t)}} |\varphi_k^{(m,t)}\rangle.\end{aligned}\quad (32)$$

Thus, by applying of the u_{mk} unitaries for the total evolution time T , $\tilde{X} \in \mathbb{C}^{M \times T}$ is as

$$\begin{aligned}\tilde{X} &= U_B W \\ &= \sum_{m=1}^M \sum_{k=1}^K \ell_{m,k}(\tau) |k_m\rangle, \\ &= \alpha \left(\sum_{k_1=1}^{K_1} |k_1\rangle + \dots + \sum_{k_M=1}^{K_M} |k_M\rangle \right),\end{aligned}\quad (33)$$

where K_m is the number of bases associated with the m -th source system,

$$\sum_{m=1}^K K_m = K, \tag{34}$$

and $0 \leq |\ell_{m,k}(\tau)|^2 \leq 1, \sum_{m=1}^M \sum_{k=1}^K |\ell_{m,k}(\tau)|^2 = 1$.

In our setting $M = 2$, and our aim is to get the system state $m = 1$ on the output of the HRE quantum memory, thus a $|\Phi^*\rangle$ target output system state is defined as

$$|\Phi^*\rangle = \frac{1}{\sqrt{K_1}} \sum_{k_1=1}^{K_1} |k_1\rangle, \tag{35}$$

where K_1 is the number of bases for source system $m = 1, k_1 = 1, \dots, K_1$.

Let rewrite the system state \tilde{X} (32) as

$$\tilde{X} = \left\{ \tilde{X}^{(1,t)}, \dots, \tilde{X}^{(M,t)} \right\}_{t=1}^T, \tag{36}$$

and let

$$X^{(t)} = \sum_{m=1}^M X^{(m,t)}, \tag{37}$$

and

$$\tilde{X}^{(t)} = \sum_{m=1}^M \tilde{X}^{(m,t)}. \tag{38}$$

Then, let $\rho_{\vec{X}}$ be a density matrix associated with \vec{X} , defined as

$$\rho_{\vec{X}} = \sum_{m=1}^M \sum_{t=1}^T \tilde{X}^{(m,t)} \left(\vec{X}^{(m,t)} \right)^\dagger \tag{39}$$

and let

$$\rho_{\tilde{X}} = \sum_{m=1}^M \sum_{t=1}^T \tilde{X}^{(m,t)} \left(\tilde{X}^{(m,t)} \right)^\dagger \tag{40}$$

be the density matrix associated with (36).

The aim of the estimation is to minimize the $D(\cdot \| \cdot)$ quantum relative entropy function taken between $\rho_{\vec{X}}$ and $\rho_{\tilde{X}}$, thus an $f(U_F)$ objective function for U_F is defined via (37) and (38) as

$$\begin{aligned} f(U_F) &= \min_{\tilde{X}} D(\rho_{\vec{X}} \| \rho_{\tilde{X}}) \\ &= \min_{\tilde{X}} \text{Tr}(\rho_{\vec{X}} \log(\rho_{\vec{X}})) - \text{Tr}(\rho_{\vec{X}} \log(\rho_{\tilde{X}})). \end{aligned} \tag{41}$$

To achieve the objective function $f(U_F)$ in (41), a factorization method is defined for U_F that is based on the fundamentals of Bayesian nonnegative matrix factorization¹¹⁸⁻¹²⁷ (Footnote: The U_F factorization unitary applied on the mixed state of the quantum register is analogous to a Poisson-Exponential Bayesian nonnegative matrix factorization¹¹⁸⁻¹²¹ process). The method adopts the Poisson distribution as $\mathcal{L}(\cdot)$ likelihood function and the exponential distribution for the control parameters¹¹⁸⁻¹²¹ α_{mk} and β_{kt} defined for the controlling of u_{mk} and w_{kt} .

Let u_{mk} and w_{kt} from (29) be defined via the control parameters α_{mk} and β_{kt} as exponential distributions

$$u_{mk} \simeq \alpha_{mk} e^{-\alpha_{mk} u_{mk}}, \tag{42}$$

with mean α_{mk}^{-1} , and

$$w_{kt} \simeq \beta_{kt} e^{-\beta_{kt} w_{kt}}, \tag{43}$$

with mean β_{kt}^{-1} .

Using (41), (42) and (43), a $\mathcal{L}(\cdot)$ log likelihood function

$$-\mathcal{L}(x, y|z) = -\log \text{Pr}(x, y|z) \tag{44}$$

can be defined as

$$\begin{aligned}
 & -\mathcal{L}(U_B, W|\vec{X}) \\
 & = D(\rho_{\vec{X}}||\rho_{\tilde{X}}) + \sum_{m=1}^M \sum_{k=1}^K \alpha_{mk} \mathbf{u}_{mk} (\alpha_{mk} \mathbf{u}_{mk})^\dagger \\
 & \quad + \sum_{k=1}^K \sum_{t=1}^T \beta_{kt} \mathbf{w}_{kt} (\beta_{kt} \mathbf{w}_{kt})^\dagger,
 \end{aligned} \tag{45}$$

thus the objective function $f(U_F)$ can be rewritten via as (45)

$$f(U_F) = \min_{\vec{X}} (-\mathcal{L}(U_B, W|\vec{X})). \tag{46}$$

The problem is therefore can be reduced to determine the model parameters

$$\zeta = \{U_B, W\} \tag{47}$$

that are treated as latent variables for the estimation of the control parameters^{118–121,125–127}

$$\tau_{mk}^{(t)} = \{\alpha_{mk}, \beta_{kt}\}. \tag{48}$$

A maximum likelihood estimation $\tilde{\zeta}$ of (47) is as

$$\tilde{\zeta} = \arg \max_{\zeta} \mathcal{D}(\vec{X}|\zeta), \tag{49}$$

where $\mathcal{D}(\cdot)$ is some distribution, that identifies an incomplete estimation problem.

The estimation of (47) can also be yielded from a maximization of a marginal likelihood function $\mathcal{L}(\vec{X}|\zeta)$ as

$$\mathcal{L}(\vec{X}|\zeta) = \int \int \sum_{\vec{\kappa}} \mathcal{D}(\vec{X}|\vec{\kappa}) \mathcal{D}(\vec{\kappa}|U_B, W) \mathcal{D}(U_B, W|\zeta) dU_B dW, \tag{50}$$

where $\vec{\kappa}$ is a complex matrix, $\vec{\kappa} \in \mathbb{C}^{M \times T}$,

$$\vec{\kappa} = \{\kappa^{(1,t)}, \dots, \kappa^{(M,t)}\}_{t=1}^T, \tag{51}$$

where

$$\kappa^{(m,t)} = (\kappa_{k=1}^{(m,t)}, \dots, \kappa_{k=K}^{(m,t)})^T, \tag{52}$$

with

$$\kappa_k^{(m,t)} = \kappa_{mkt} \tag{53}$$

where

$$\kappa_{mkt} = \mathbf{u}_{mk} \mathbf{w}_{kt}. \tag{54}$$

The quantity in (54) can be estimated via (42) and (43) as

$$\kappa_{mkt} \approx \alpha_{mk} e^{-\alpha_{mk} \mathbf{u}_{mk}} \beta_{kt} e^{-\beta_{kt} \mathbf{w}_{kt}}. \tag{55}$$

Using (54), $\tilde{X}^{(m,t)}$ in (29) can be rewritten as

$$\tilde{X}^{(m,t)} = \sum_{m=1}^M \sum_{k=1}^K \kappa_{mkt}. \tag{56}$$

However, since the exact solution does not exists^{118–121}, since it would require the factorization of $\mathcal{D}(\vec{\kappa}, U_B, W|\vec{X}, \zeta)$, such that ζ, U_B, W are unknown.

This problem can be solved by a variational Bayesian inference procedure^{118–121,125–127}, via the maximization of the lower bound of a likelihood function $\mathcal{L}_{\mathcal{Q}_v}$

$$\begin{aligned}
 \mathcal{L}_{\mathcal{Q}_v} & = \iint \sum_{\vec{\kappa}} \mathcal{Q}_v(\vec{\kappa}, U_B, W) \log \frac{\mathcal{D}(\vec{X}, \vec{\kappa}, U_B, W|\zeta)}{\mathcal{Q}_v(\vec{\kappa}, U_B, W)} dU_B dW \\
 & = \mathbb{E}(\log \mathcal{D}(\vec{X}, \vec{\kappa}, U_B, W|\zeta)) + H(\mathcal{Q}_v(\vec{\kappa}, U_B, W)),
 \end{aligned} \tag{57}$$

where \mathcal{Q}_v is a variational distribution, while $H(\mathcal{Q}_v(\vec{\kappa}, U_B, W))$ is the entropy of variational distribution $\mathcal{Q}_v(\vec{\kappa}, U_B, W)$,

$$H(\mathcal{D}_v(\vec{\kappa}, U_B, W)) = \sum_{m=1}^M \sum_{t=1}^T H(\kappa^{(m,t)}) + \sum_{m=1}^M \sum_{k=1}^K H(u_{mk}) + \sum_{k=1}^K \sum_{t=1}^T H(w_{kt}), \tag{58}$$

and where $\mathcal{D}_v(\vec{\kappa}, U_B, W)$ is a joint variational distribution, as

$$\begin{aligned} \mathcal{D}_v(\vec{\kappa}, U_B, W) &= \mathcal{D}_v(\vec{\kappa}) \mathcal{D}_v(U_B) \mathcal{D}_v(W) \\ &= \prod_m \prod_t \prod_k \mathcal{D}_v(\kappa_{mkt}) \mathcal{D}_v(u_{mk}) \mathcal{D}_v(w_{kt}), \end{aligned} \tag{59}$$

from which distribution $\mathcal{D}(\vec{\kappa}, U_B, W | \vec{X}, \zeta)$ can be approximated as^{118–121}

$$\mathcal{D}(\vec{\kappa}, U_B, W | \vec{X}, \zeta) \approx \prod_m \prod_t \prod_k \mathcal{D}_v(\kappa_{mkt}) \mathcal{D}_v(u_{mk}) \mathcal{D}_v(w_{kt}). \tag{60}$$

The function $\mathcal{L}_{\mathcal{D}_v}$ in (57) is related to (50) as

$$\mathcal{L}(\vec{X} | \zeta) \geq \mathcal{L}_{\mathcal{D}_v}. \tag{61}$$

The result in (59) therefore also determines the number K of bases selected for the factorization unitary U_F . The \mathcal{D}_v variational distributions $\mathcal{D}_v(\kappa_{mkt})$, $\mathcal{D}_v(u_{mk})$ and $\mathcal{D}_v(w_{kt})$ are determined for the unitary U_F as follows.

Let $\mathcal{D}_v(\Phi)$ refer to the variational distribution of a given Φ ,

$$\Phi \in \{\vec{\kappa}, U_B, W\}. \tag{62}$$

Since only the joint (posterior) distribution $\mathcal{D}(\vec{X}, \vec{\kappa}, U_B, W | \zeta)$ is obtainable, the variational distributions have to be evaluated as

$$\mathbb{E}_{\mathcal{D}_v(i \neq \Phi)}(\log \mathcal{D}(\vec{X}, \vec{\kappa}, U_B, W | \zeta)) = \log \mathcal{D}_v(\Phi), \tag{63}$$

where $\mathbb{E}_{\mathcal{D}_v(i \neq \Phi)}(\cdot)$ is the expectation function of the $\mathcal{D}_v(i)$ variational distribution of i , such that $i \neq \Phi$, where Φ is as in (62), with

$$\mathbb{E}_a(f(a) + g(a)) = \mathbb{E}_a(f(a)) + \mathbb{E}_a(g(a)), \tag{64}$$

for some functions $f(a)$ and $g(a)$, and

$$\mathbb{E}_a(bf(a)) = b\mathbb{E}_a(f(a)) \tag{65}$$

for some constant b , (note: for simplicity, we use $\mathbb{E}(\cdot)$ for the expectation function), while

$$\begin{aligned} &\log \mathcal{D}(\vec{X}, \vec{\kappa}, U_B, W | \zeta) \\ &= \sum_{m=1}^M \sum_{t=1}^T \log f_\delta \left(X^{(m,t)} - \sum_{k=1}^K \kappa_{mkt} \right) + \sum_{m=1}^M \sum_{k=1}^K \sum_{t=1}^T (\kappa_{mkt} \log(u_{mk} w_{kt}) \\ &\quad - u_{mk} w_{kt} - \log f_\Gamma(\kappa_{mkt} + 1)) + \sum_{m=1}^M \sum_{k=1}^K (\log \alpha_{mk} - \alpha_{mk} u_{mk}) \\ &\quad + \sum_{k=1}^K \sum_{t=1}^T (\log \beta_{kt} - \beta_{kt} w_{kt}), \end{aligned} \tag{66}$$

where $f_\delta(\cdot)$ is the Dirac delta function, while $f_\Gamma(\cdot)$ is the Gamma function,

$$f_\Gamma(x) = \int_0^\infty t^{x-1} e^{-t} dt. \tag{67}$$

By utilizing a variational Poisson–Exponential Bayesian learning^{118–121}, these variational distributions can be evaluated as follows.

The $\mathcal{D}_v(\kappa_{mkt})$ variational distribution is as

$$\mathcal{D}_v(\kappa_{mkt}) = \mathcal{M}(\kappa_{mkt} | \eta_{mkt}) \tag{68}$$

where \mathcal{M} is a multinomial distribution, while η_{mkt} is a multinomial parameter

$$\eta_{mkt} = \frac{e^{\mathbb{E}(\log u_{mk}) + \mathbb{E}(\log w_{kt})}}{\sum_j e^{\mathbb{E}(\log u_{mj}) + \mathbb{E}(\log w_{jt})}}, \tag{69}$$

while the $\mathcal{D}_v(\kappa^{(m,t)})$ variational distribution is as

$$\begin{aligned} & \mathcal{M}(\kappa^{(m,t)} | X^{(m,t)}, \eta_k^{(m,t)}) \\ &= f_\delta \left(X^{(m,t)} - \sum_{k=1}^K \kappa_{mkt} \right) X^{(m,t)}! \prod_k \frac{(\eta_{mkt})^{\kappa_{mkt}}}{\kappa_{mkt}!}, \end{aligned} \tag{70}$$

where $\eta_k^{(m,t)}$ is a multinomial parameter vector

$$\eta_k^{(m,t)} = (\eta_{k=1}^{(m,t)}, \dots, \eta_{k=K}^{(m,t)})^T, \tag{71}$$

such that

$$\sum_{k=1}^K \eta_k^{(m,t)} = 1. \tag{72}$$

The $\mathcal{D}_v(u_{mk})$ variational distribution is as

$$\begin{aligned} & \mathcal{D}_v(u_{mk}) \\ &= e^{\left(\sum_{t=1}^T \mathbb{E}(\kappa_{mkt}) \log u_{mk} - \left(\sum_{t=1}^T \mathbb{E}(w_{kt}) + \alpha_{mk} \right) u_{mk} \right)} \\ &= \mathcal{G}(u_{mk} | \tilde{\alpha}_{mk}(A), \tilde{\alpha}_{mk}(B)), \end{aligned} \tag{73}$$

where $\mathcal{G}(\cdot)$ is a Gamma distribution,

$$\mathcal{G}(x; a, b) = e^{(a-1)\log x - \frac{x}{b} - \log \Gamma(a) - a \log b}, \tag{74}$$

where a is a shape parameter, while b is a scale parameter, $\Gamma(\cdot)$ is the Gamma function (67). The entropy of (74) is as

$$H(\mathcal{G}(x; a, b)) = -(a - 1) \partial_{\mathcal{G}_{\log}}(a) + \log b + a + \log \Gamma(a), \tag{75}$$

where $\partial_{\mathcal{G}_{\log}}(\cdot)$ is the derivative of the log gamma function (digamma function),

$$\partial_{\mathcal{G}_{\log}}(x) = \frac{d \log \Gamma(x)}{dx}, \tag{76}$$

while $\mathbb{E}(\kappa_{mkt})$ is evaluated as

$$\mathbb{E}(\kappa_{mkt}) = X^{(m,t)} \eta_{mkt}, \tag{77}$$

while $\tilde{\alpha}_{mk}(A)$ and $\tilde{\alpha}_{mk}(B)$ are control parameters for U_b , defined as

$$\tilde{\alpha}_{mk}(A) = 1 + \sum_{t=1}^T \mathbb{E}(\kappa_{mkt}), \tag{78}$$

while $\tilde{\alpha}_{mk}(B)$ is defined as

$$\tilde{\alpha}_{mk}(B) = \frac{1}{\sum_{t=1}^T \mathbb{E}(w_{kt}) + \alpha_{mk}}. \tag{79}$$

The $\mathcal{D}_v(w_{kt})$ variational distribution is as

$$\begin{aligned} & \mathcal{D}_v(w_{kt}) \\ &= e^{\left(\sum_{m=1}^M \mathbb{E}(\kappa_{mkt}) \log w_{kt} - \left(\sum_{m=1}^M \mathbb{E}(u_{mk}) + \beta_{kt} \right) w_{kt} \right)} \\ &= \mathcal{G}(w_{kt} | \tilde{\beta}_{kt}(A), \tilde{\beta}_{kt}(B)), \end{aligned} \tag{80}$$

where $\tilde{\beta}_{kt}(A)$ and $\tilde{\beta}_{kt}(B)$ are control parameters for W , defined as

$$\tilde{\beta}_{kt}(A) = 1 + \sum_{m=1}^M \mathbb{E}(\kappa_{mkt}), \tag{81}$$

and

$$\tilde{\beta}_{kt}(B) = \frac{1}{\sum_{m=1}^M \mathbb{E}(u_{mk}) + \beta_{kt}}. \tag{82}$$

Given the variational parameters $\tilde{\alpha}_{mk}(A), \tilde{\alpha}_{mk}(B), \tilde{\beta}_{kt}(A)$ and $\tilde{\beta}_{kt}(B)$ in (78), (79), (81) and (82), the estimates of U_B and W are realized by the determination of the Gamma means $\mathbb{E}(u_{mk})$ and $\mathbb{E}(w_{kt})$ ^{118–121}. It can be verified that the mean $\mathbb{E}(w_{kt})$ in (73), (79) and (80) can be evaluated via (81) and (82) as a mean of a Gamma distribution

$$\mathbb{E}(w_{kt}) = \tilde{\beta}_{kt}(A)\tilde{\beta}_{kt}(B), \tag{83}$$

while $\mathbb{E}(\log w_{kt})$ is as

$$\mathbb{E}(\log w_{kt}) = \partial_{\mathcal{G}_{\log}}(\tilde{\beta}_{kt}(A)) + \log \tilde{\beta}_{kt}(B), \tag{84}$$

where $\partial_{\mathcal{G}_{\log}}(\cdot)$ digamma function (76).

The mean $\mathbb{E}(u_{mk})$ in (80) and (82) can be evaluated via (78) and (79), as a mean of a Gamma distribution

$$\mathbb{E}(u_{mk}) = \tilde{\alpha}_{mk}(A)\tilde{\alpha}_{mk}(B), \tag{85}$$

and $\mathbb{E}(\log u_{mk})$ is yielded as

$$\mathbb{E}(\log u_{mk}) = \partial_{\mathcal{G}_{\log}}(\tilde{\alpha}_{mk}(A)) + \log \tilde{\alpha}_{mk}(B). \tag{86}$$

As the $\mathcal{D}_v(\kappa_{mkt}), \mathcal{D}_v(u_{mk})$ and $\mathcal{D}_v(w_{kt})$ variational distributions are determined via (68), (73) and (80) the evaluation of (59) is straightforward.

Using the defined terms, the term $\mathbb{E}(\log \mathcal{D}(\vec{X}, \vec{\kappa}, U_B, W|\zeta))$ from (57) can be evaluated as

$$\begin{aligned} & \mathbb{E}(\log \mathcal{D}(\vec{X}, \vec{\kappa}, U_B, W|\zeta)) \\ &= \sum_{m=1}^M \sum_{t=1}^T \mathbb{E} \left(\log f_{\delta} \left(X^{(m,t)} - \sum_{k=1}^K \kappa_{mkt} \right) \right) \\ &+ \sum_{m=1}^M \sum_{k=1}^K \mathbb{E}(\log u_{mk}) \sum_{t=1}^T \mathbb{E}(\kappa_{mkt}) \\ &+ \sum_{k=1}^K \sum_{t=1}^T \mathbb{E}(\log w_{kt}) \sum_{m=1}^M \mathbb{E}(\kappa_{mkt}) - \sum_{m=1}^M \sum_{k=1}^K \sum_{t=1}^T \mathbb{E}(u_{mk}) \mathbb{E}(w_{kt}) \\ &- \sum_{m=1}^M \sum_{k=1}^K \sum_{t=1}^T \mathbb{E}(\log f_{\Gamma}(\kappa_{mkt} + 1)) \\ &+ \sum_{m=1}^M \sum_{k=1}^K (\log \alpha_{mk} - \alpha_{mk} \mathbb{E}(u_{mk})) \\ &+ \sum_{k=1}^K \sum_{t=1}^T (\log \beta_{kt} - \beta_{kt} \mathbb{E}(w_{kt})), \end{aligned} \tag{87}$$

while the $H(\mathcal{D}_v(\vec{\kappa}, U_B, W))$ entropy of the variational distribution from (58) can be evaluated as

$$\begin{aligned} & H(\mathcal{D}_v(\vec{\kappa}, U_B, W)) \\ &= \sum_{m=1}^M \sum_{t=1}^T \left(-\log f_{\Gamma}(X^{(m,t)} + 1) - \sum_{k=1}^K \mathbb{E}(\kappa_{mkt}) \log \eta_{mkt} \right) \\ &+ \sum_{m=1}^M \sum_{k=1}^K \sum_{t=1}^T \mathbb{E}(\log f_{\Gamma}(\kappa_{mkt} + 1)) \\ &- \sum_{m=1}^M \sum_{t=1}^T \mathbb{E} \left(\log f_{\delta} \left(X^{(m,t)} - \sum_{k=1}^K \kappa_{mkt} \right) \right) \\ &+ \sum_{m=1}^M \sum_{k=1}^K (-\tilde{\alpha}_{mk}(A) - 1) \partial_{\mathcal{G}_{\log}}(\tilde{\alpha}_{mk}(A)) + \log(\tilde{\alpha}_{mk}(B)) \\ &+ \tilde{\alpha}_{mk}(A) + \log f_{\Gamma}(\tilde{\alpha}_{mk}(A)) \\ &+ \sum_{k=1}^K \sum_{t=1}^T (-\tilde{\beta}_{kt}(A) - 1) \partial_{\mathcal{G}_{\log}}(\tilde{\beta}_{kt}(A)) + \log(\tilde{\beta}_{kt}(B)) \\ &+ \tilde{\beta}_{kt}(A) + \log f_{\Gamma}(\tilde{\beta}_{kt}(A)). \end{aligned} \tag{88}$$

Thus, from (87) and (88), the lower bound $\mathcal{L}_{\mathcal{D}_v}$ in (57) is as

$$\begin{aligned}
 \mathcal{L}_{\mathcal{D}_v} = & -\sum_{m=1}^M \sum_{t=1}^T \sum_{k=1}^K \mathbb{E}(u_{mk}) \mathbb{E}(w_{kt}) \\
 & + \sum_{m=1}^M \sum_{t=1}^T \left(-\log f_{\Gamma}(X^{(m,t)} + 1) - \sum_{k=1}^K \mathbb{E}(\kappa_{mkt}) \log \eta_{mkt} \right) \\
 & + \sum_{m=1}^M \sum_{k=1}^K \mathbb{E}(\log u_{mk}) \sum_{t=1}^T \mathbb{E}(\kappa_{mkt}) \\
 & + \sum_{k=1}^K \sum_{t=1}^T \mathbb{E}(\log w_{kt}) \sum_{m=1}^M \kappa_{mkt} \\
 & + \sum_{m=1}^M \sum_{k=1}^K (\log \alpha_{mk} - \alpha_{mk} \mathbb{E}(u_{mk})) \\
 & + \sum_{k=1}^K \sum_{t=1}^T (\log \beta_{kt} - \beta_{kt} \mathbb{E}(w_{kt})) \\
 & + \sum_{m=1}^M \sum_{k=1}^K (-(\tilde{\alpha}_{mk}(A) - 1) \partial_{\mathcal{G}_{\log}}(\tilde{\alpha}_{mk}(A)) + \log \tilde{\alpha}_{mk}(B) \\
 & + \tilde{\alpha}_{mk}(A) + \log f_{\Gamma}(\tilde{\alpha}_{mk}(A))) \\
 & + \sum_{k=1}^K \sum_{t=1}^T (-(\tilde{\beta}_{kt}(A) - 1) \partial_{\mathcal{G}_{\log}}(\tilde{\beta}_{kt}(A)) + \log \tilde{\beta}_{kt}(B) \\
 & + \tilde{\beta}_{kt}(A) + \log f_{\Gamma}(\tilde{\beta}_{kt}(A))).
 \end{aligned} \tag{89}$$

The next problem is the $\tilde{\tau}_k^{(t)}$ estimation of the control parameters α_{mk}, β_{kt} in (48) as

$$\tilde{\tau}_{mk}^{(t)} = \{E_{mk}, F_{kt}\}, \tag{90}$$

such that E_{mk} is a basis estimation

$$E_{mk} \approx \alpha_{mk} \tag{91}$$

and F_{kt} is a system estimation

$$F_{kt} \approx \beta_{kt}, \tag{92}$$

such that the variational lower bound $\mathcal{L}_{\mathcal{D}_v}$ in (89) is maximized¹¹⁸⁻¹²¹. It is achieved for the unitary U_F as follows. The maximization problem can be formalized via the $\partial(\mathcal{L}_{\mathcal{D}_v})$ derivative of $\mathcal{L}_{\mathcal{D}_v}$

$$\frac{\partial(\mathcal{L}_{\mathcal{D}_v})}{\partial \alpha_{mk}} = \frac{1}{\alpha_{mk}} - \mathbb{E}(u_{mk}) + \frac{\partial(\log(\tilde{\alpha}_{mk}(B)))}{\partial \alpha_{mk}} = 0, \tag{93}$$

and

$$\frac{\partial(\mathcal{L}_{\mathcal{D}_v})}{\partial \beta_{kt}} = \frac{1}{\beta_{kt}} - \mathbb{E}(w_{kt}) + \frac{\partial(\log(\tilde{\beta}_{kt}(B)))}{\partial \beta_{kt}} = 0, \tag{94}$$

which is solvable via^{118,120}

$$(\alpha_{mk})^2 + \sum_{t=1}^T \mathbb{E}(w_{kt}) \alpha_{mk} - \frac{\sum_{t=1}^T \mathbb{E}(w_{kt})}{\mathbb{E}(u_{mk})} = 0, \tag{95}$$

and

$$(\beta_{kt})^2 + \sum_{m=1}^M \mathbb{E}(u_{mk}) \beta_{kt} - \frac{\sum_{m=1}^M \mathbb{E}(u_{mk})}{\mathbb{E}(w_{kt})} = 0. \tag{96}$$

After some calculations, E_{mk} and F_{kt} from (90) are as

$$E_{mk} = \frac{1}{2} \left(-\sum_{t=1}^T \mathbb{E}(w_{kt}) + \left(\left(\sum_{t=1}^T \mathbb{E}(w_{kt}) \right)^2 + 4 \frac{\sum_{t=1}^T \mathbb{E}(w_{kt})}{\mathbb{E}(u_{mk})} \right)^{\frac{1}{2}} \right), \tag{97}$$

and

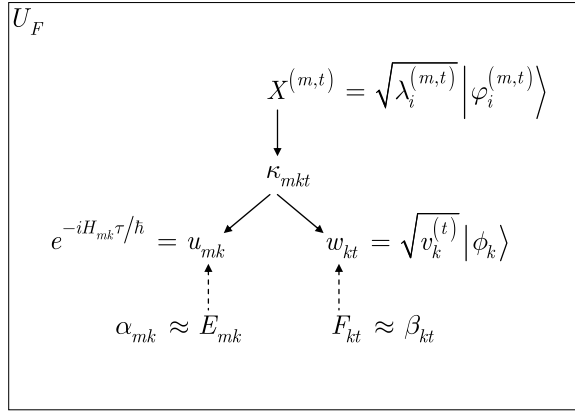


Figure 3. Representation of the U_F unitary over a total evolution time t , with K factored bases and M source systems ($M = 2$ in our setting). The factorization is represented by the solid-line arrows. At a given t , $t = 1, \dots, T$, the input system of U_F subject of factorization is $X^{(m,t)} = \sqrt{\lambda_i^{(m,t)}} |\phi_i^{(m,t)}\rangle$, $m = 1, \dots, M$. Term κ_{mkt} is expressed as $\kappa_{mkt} = u_{mk}w_{kt}$, where $u_{mk} = e^{-iH_{mk}\tau/\hbar}$ is a unitary, $u_{mk} \in \mathbb{C}$, $k = 1, \dots, K$, which sets a computational basis for w_{kt} , $w_{kt} = W_k^{(t)} = \sqrt{v_k^{(t)}} |\phi_k\rangle$. The basis matrix is $U_B = \{u_{mk}\} \in \mathbb{C}^{M \times K}$ with K bases, $H_{mk} = G_{mk}|k_m\rangle\langle k_m|$ is a Hamiltonian, and $W = \{W_k^{(t)} = w_{kt}\} \in \mathbb{C}^{K \times T}$, $w_{kt} \in \mathbb{C}$. The factorization decomposes $X^{(m,t)}$ into $X^{(m,t)} = [U_B \vec{W}]_{mt}$, and for the total evolution $\vec{X} = U_B \vec{W}$, where $\vec{X} = \{X^{(1,t)}, \dots, X^{(M,t)}\}_{t=1}^T$, while κ_{kt} is as $\kappa_{mkt} = u_{mk}w_{kt}$. Terms α_{mk} and β_{kt} are control parameters for u_{mk} and w_{kt} (controlling is depicted by the dashed-line arrows) to evaluate the parameters as $u_{mk} \simeq \alpha_{mk} e^{-\alpha_{mk} u_{mk}}$ and $w_{kt} \simeq \beta_{kt} e^{-\beta_{kt} w_{kt}}$, estimated by E_{mk} and F_{kt} as $\tilde{u}_{mk} = E_{mk} e^{-E_{mk} \tilde{u}_{mk}}$ and $\tilde{w}_{kt} = F_{kt} e^{-F_{kt} \tilde{w}_{kt}}$.

$$F_{kt} = \frac{1}{2} \left[\sum_{m=1}^M \mathbb{E}(u_{mk}) + \left(\left(\sum_{m=1}^M \mathbb{E}(u_{mk}) \right)^2 + 4 \frac{\sum_{m=1}^M \mathbb{E}(u_{mk})}{\mathbb{E}(w_{kt})} \right)^{\frac{1}{2}} \right], \tag{98}$$

respectively.

From (97) and (98), the $\tilde{\tau}_{mk}^{(t)}$ estimation in (90) is therefore straightforwardly yielded. Therefore, using the parameters $\tilde{\alpha}_{mk}(B)$, $\tilde{\alpha}_{mk}(A)$, $\tilde{\beta}_{kt}(B)$ and η_{mkt} , the optimal variational distributions $\mathcal{D}_v(\kappa_{mkt})$, $\mathcal{D}_v(u_{mk})$ and $\mathcal{D}_v(w_{kt})$ can be substituted to estimate $\tilde{\tau}_{mk}^{(t)}$.

Using (97) and (98), the estimation of terms u_k (42), w_{kt} (43) and κ_{kt} (55) are yielded as

$$\tilde{u}_{mk} = E_{mk} e^{-E_{mk} \tilde{u}_{mk}}, \tag{99}$$

$$\tilde{w}_{kt} = F_{kt} e^{-F_{kt} \tilde{w}_{kt}}, \tag{100}$$

and

$$\tilde{\kappa}_{mkt} = E_{mk} e^{-E_{mk} \tilde{u}_{mk}} F_{kt} e^{-F_{kt} \tilde{w}_{kt}}. \tag{101}$$

The evaluation of (97) and (98) therefore is yielded in an iterative manner through the $\tilde{\alpha}_{mk}(B)$, $\tilde{\alpha}_{mk}(A)$, $\tilde{\beta}_{kt}(A)$, $\tilde{\beta}_{kt}(B)$ and η_{mkt} , and the K^* optimal number of bases, K , is determined with respect to (89) such that

$$K^* = \underset{K}{\operatorname{argmax}} \mathcal{L}_{\mathcal{D}_v}(K), \tag{102}$$

where $\mathcal{L}_{\mathcal{D}_v}(K)$ refers to $\mathcal{L}_{\mathcal{D}_v}$ from (89) at a particular base number K .

The proof is concluded here. ■

The schematic representation of unitary U_F is depicted in Fig. 3.

Quantum constant Q transform. As the $\{\tilde{u}_{mk}\}$ basis estimations (99) are determined via $\{E_{mk}\}$ (97), the next problem is the partitioning of the K bases with respect to M , see (8). To achieve the partitioning, first the bases of U_B are transformed by the U_{CQT} is the quantum constant Q transform¹²⁸. The U_{CQT} operation is similar to the discrete QFT (quantum Fourier transform) transform¹¹⁷, and defined in the following manner.

The U_{CQT} transform is defined as

$$U_{CQT}(|k\rangle, m) = \frac{1}{\sqrt{N}} \sum_{j=0}^{N-1} f_W(j - m) e^{2\pi i j Q/m} |j\rangle = |\phi_k\rangle, \tag{103}$$

where $|k\rangle$ is a quantum state of the computational basis B , and in the current setting

$$N = K, \tag{104}$$

and

$$|k\rangle = E_{mk}, \tag{105}$$

thus B is as

$$B: \{|0\rangle, \dots, |K - 1\rangle\}, \tag{106}$$

while h is selected such that

$$0 \leq (j - h) \leq N - 1 = K - 1 \tag{107}$$

holds, and Q is defined via the following relation

$$\frac{2\pi k}{K} = \frac{2\pi Q}{h}, \tag{108}$$

from which Q is yielded at a given h, k and K , as

$$Q = \frac{hk}{K}, \tag{109}$$

while $f_W(\cdot)$ is a windowing function¹²⁹ that localizes the wavefunctions of the quantum register, defined via parameter h as

$$f_W(j - h) = \frac{1}{2} \left(1 - \cos \left(\frac{2\pi(h - m)}{K - 1} \right) \right). \tag{110}$$

(Footnote: The function in (110) is the so-called Hanning window¹²⁹.)

The $|\phi_k\rangle$ output states of U_{CQT} therefore identify a set \mathcal{S}_ϕ of states, as

$$\mathcal{S}_\phi: \{|\phi_k\rangle: k = 0, \dots, K - 1\} \tag{111}$$

that formulates an orthonormal basis.

The U_{CQT}^\dagger inverse of U_{CQT} will be processed as the U_p partitioning is completed, with the same $f_W(\cdot)$ windowing function, defined as

$$U_{CQT}^\dagger(|k\rangle, h) = \frac{1}{\sqrt{K}} \sum_{j=0}^{K-1} f_W(j - h) e^{-2\pi i j Q/h} |j\rangle. \tag{112}$$

Applying (103) on the K estimated bases $\{E_{mk}\}$ yields the C_B transformed bases, as

$$\begin{aligned} C_B &= U_{CQT}(U_B) \\ &= \{C_{mk}\} \in \mathbb{C}^{M \times K}, \end{aligned} \tag{113}$$

where C_{mk} is as,

$$C_{mk} = U_{CQT}(E_{mk}). \tag{114}$$

After the application of (113), the resulting system is therefore as

$$C_B W = (U_{CQT} U_B) W, \tag{115}$$

where $C_B W \in \mathbb{C}^{M \times T}$.

Basis partitioning unitary. Theorem 2. (Partitioning the bases of source systems). *The Q transformed bases can be partitioned to M partitions via the U_p partitioning unitary operation.*

Proof. As the U_{CQT} transforms of the $\{E_{mk}\}$ basis estimations (99) are determined via C_B (113), the Q transformed bases are partitioned to M partitions via the U_p unitary operation, as follows.

Let the system state from (115) be denoted by

$$S = C_B W \tag{116}$$

and let \tilde{S} be the estimation of S ¹³⁰, defined as

$$\tilde{S} = \langle\langle \mathcal{R}\mathcal{E}\mathcal{H} \rangle\rangle, \quad (117)$$

where

$$\mathcal{T} \in \{\mathcal{R}, \mathcal{E}, \mathcal{H}\} \quad (118)$$

is a tensor (multidimensional array)^{131,132} with dimension $\dim(\mathcal{T})$, and size

$$s(\mathcal{T}) = \prod_{i=1}^{\dim(\mathcal{T})} |d_i(\mathcal{T})|, \quad (119)$$

where $|d_i(\mathcal{T})|$ is the size of the i -th dimension $d_i(\mathcal{T})$.

Let

$$\mathcal{R} = \mathcal{A} \circ \mathcal{B} \quad (120)$$

be a translation tensor of size

$$\begin{aligned} s(\mathcal{R}) &= \prod_{i=1}^{\dim(\mathcal{R})} |d_i(\mathcal{R})| \\ &= \prod_{i=1}^{\dim(\mathcal{A})} |d_i(\mathcal{A})| \times \prod_{i=1}^{\dim(\mathcal{B})} |d_i(\mathcal{B})|, \end{aligned} \quad (121)$$

with

$$\dim(\mathcal{R}) = 3, \quad (122)$$

as

$$|d_1(\mathcal{R})| = M, \quad (123)$$

$$|d_2(\mathcal{R})| = 1, \quad (124)$$

and

$$|d_3(\mathcal{R})| = M \quad (125)$$

and let

$$\mathcal{E} = \mathcal{A} \circ \mathcal{C} \quad (126)$$

be a tensor of size

$$\begin{aligned} s(\mathcal{E}) &= \prod_{i=1}^{\dim(\mathcal{E})} |d_i(\mathcal{E})| \\ &= \prod_{i=1}^{\dim(\mathcal{A})} |d_i(\mathcal{A})| \times \prod_{i=1}^{\dim(\mathcal{C})} |d_i(\mathcal{C})|, \end{aligned} \quad (127)$$

with

$$\dim(\mathcal{E}) = 2 \quad (128)$$

as

$$|d_1(\mathcal{E})| = M, \quad (129)$$

$$|d_2(\mathcal{E})| = K, \quad (130)$$

and with

$$\dim(\mathcal{H}) = 3, \quad (131)$$

as

$$|d_1(\mathcal{H})| = 1, \quad (132)$$

$$|d_2(\mathcal{H})| = K \quad (133)$$

and

$$|d_3(\mathcal{R})| = T, \quad (134)$$

thus

$$\dim(\mathcal{A}) = M \quad (135)$$

and

$$\dim(\mathcal{B}) = M \quad (136)$$

while

$$\dim(\mathcal{C}) = K. \quad (137)$$

The term $\langle \mathcal{R}\mathcal{E} \rangle$ is evaluated as

$$\begin{aligned} & \langle \mathcal{R}\mathcal{E} \rangle_{\{1:\dim(\mathcal{A}), 1:\dim(\mathcal{B})\}}(j_1, \dots, j_{\dim(\mathcal{B})}, k_1, \dots, k_{\dim(\mathcal{C})}) \\ &= \sum_{i_1=1}^{d_1(\mathcal{A})} \dots \sum_{i_{\dim(\mathcal{A})}=1}^{d_{\dim(\mathcal{A})}(\mathcal{A})} \mathcal{R}(i_1, \dots, i_{\dim(\mathcal{A})}, j_1, \dots, j_{\dim(\mathcal{B})}) \\ & \quad \times \mathcal{E}(i_1, \dots, i_{\dim(\mathcal{A})}, k_1, \dots, k_{\dim(\mathcal{C})}), \end{aligned} \quad (138)$$

where $\mathcal{R}(i, j)$ is the indexing for the elements of the tensor.

Let $\mathcal{E}(\forall m, k)$ refer to the j -th column of \mathcal{E} , and let $\mathcal{H}(1, k, \forall t)$ refer to the j -th lateral slice of \mathcal{H} . Then, let be a U_p unitary operation that achieves the decomposition of (117) with respect to a given $k, k = 1, \dots, K$, as

$$[S]_k = \langle \langle \mathcal{R}\mathcal{E}(\forall m, k) \rangle \mathcal{H}(1, k, \forall t) \rangle \quad (139)$$

with a particular cost function $f(U_p)$ of the U_p unitary defined via the quantum relative entropy function, as

$$\begin{aligned} f(U_p) &= \min_{\tilde{S}} D(\rho_S \parallel \tilde{S}\tilde{S}^\dagger) \\ &= \min_{\tilde{S}} \text{Tr}(\rho_S \log(\rho_S)) - \text{Tr}(\rho_S \log(\tilde{S}\tilde{S}^\dagger)), \end{aligned} \quad (140)$$

where ρ_S is the density matrix associated with S as in (116),

$$\rho_S = U_p U_{CQT} U_F \left(\sum_{m=1}^M \sum_{t=1}^T \vec{X}^{(m,t)} \left(\vec{X}^{(m,t)} \right)^\dagger \right), \quad (141)$$

while \tilde{S} is given in (117).

Using (139), the Q -transformed bases are partitioned into M classes, the partition Ω outputted by U_p is evaluated as

$$\Omega = \arg \max_k ([Q]_k), \quad (142)$$

where Q is a $1 \times K$ size matrix, such that

$$[Q]_k = \sum_{m=1}^M \langle \langle \mathcal{R}(\forall, 1, \forall) \mathcal{E}(\forall, k) \rangle \mathcal{H}(1, k, \forall) \rangle. \quad (143)$$

Since $M = 2$ in our setting, the partition (142) can be rewritten as

$$\Omega = \Omega_Q^{(1)} + \Omega_Q^{(2)}, \quad (144)$$

where $\Omega_Q^{(m)}$ identifies a cluster of K_m Q -transformed bases for m -th system state,

$$\Omega_Q^{(m)} = \left\{ \Omega_Q^{(m, k_m)} \right\}_{k_m=1}^{K_m}, \quad (145)$$

of

$$|\Omega_Q^{(m)}| = K_m \quad (146)$$

bases formulated via the base estimations (99) for the m -th system state in (8), such that

$$\sum_{m=1}^M K_m = K. \quad (147)$$

Since the partitioning is made over the Q transformed bases, the output of U_p is then transformed by the U_{CQT}^\dagger inverse transformation (112). ■

Inverse quantum constant Q transform. Applying the U_{CQT}^\dagger inverse transformation (112) on the partitions (143) of the Q transformed bases yields the decomposition of the bases of U_B onto M classes, as

$$U_{CQT}^\dagger(\Omega) = \theta = \sum_{m=1}^M \gamma^{(m)}, \tag{148}$$

and since $M = 2$

$$\theta = \gamma^{(1)} + \gamma^{(2)}, \tag{149}$$

where $\gamma^{(m)}$ identifies a cluster of K_m bases for m -th system state.

Therefore, the resulting system state is as

$$\begin{aligned} U_{CQT}^\dagger(U_p(C_B W)) &= U_{CQT}^\dagger(U_p U_{CQT} U_B) W \\ &= \chi W. \end{aligned} \tag{150}$$

The next problem is therefore the evaluation of the estimations of the $M = 2$ source systems ρ_{in} and $\zeta_{QR}^{(t)}$, as given in (7) from χW . Using the system state (150), the system separation is produced by the U_{DSTFT}^\dagger unitary that realizes the inverse quantum DSTFT (discrete short-time Fourier transform)¹²⁹.

Inverse quantum DSTFT and quantum DFT. The result of unitary U_{ML} is evaluated further by the U_{DSTFT}^\dagger unitary.

Theorem 3. (Target source system recovery). Source system $m = 1$ can be extracted by the U_{DSTFT}^\dagger and U_{DFT} discrete quantum Fourier transform on the output of an HRE quantum memory.

Proof. The U_{DSTFT}^\dagger inverse quantum DSTFT transformation applied to a state $|k\rangle$ of the computational basis

$$B: \{|0\rangle, \dots, |K - 1\rangle\}, \tag{151}$$

is defined as

$$U_{DSTFT}^\dagger(|k\rangle, h) = \frac{1}{\sqrt{K}} \sum_{j=0}^{K-1} f_W(j - h) e^{-2\pi i j k / K} |j\rangle = |\psi_k\rangle, \tag{152}$$

where h is selected such that

$$0 \leq (j - h) \leq K - 1 \tag{153}$$

holds, set

$$\mathcal{S}_\psi: \{|\psi_k\rangle: k = 0, \dots, K - 1\} \tag{154}$$

formulates a new orthonormal basis, while $f_W(\cdot)$ is a windowing function¹²⁹.

Using system state χW in (150), let $\gamma^{(m,k)}$ be a k -th basis of cluster $\gamma^{(m)}$, and let $(\chi W)^{(m,t)}$ be defined as

$$(\chi W)^{(m,t)} = [\chi W]_{mk} = \sum_{k=1}^K \gamma^{(m,k)} W_k^{(m,t)} \tag{155}$$

and let system $|\chi W\rangle$ identify (33) as

$$|\chi W\rangle = \alpha \sum_{m=1}^M \sum_{k_m=1}^{K_m} |k_m\rangle, \tag{156}$$

where $|k_m\rangle$ is the eigenvector of the Hamiltonian of $\gamma^{(m,k_m)}$, K_m is the cardinality of cluster $\gamma^{(m)}$, while $\sum_{m=1}^M \sum_{k_m=1}^{K_m} \alpha = 1$.

Since the $|k_1\rangle$ values are some parameters of U_{ML} , we can redefine (156) as

$$|\chi W\rangle = \alpha \sum_{m=1}^M \sum_{k_m=1}^{K_m} |k_1 + x_{m,k_m}\rangle, \tag{157}$$

where

$$x_{m,k_m} = \begin{cases} 0, & \text{if } m = 1 \\ \neq 0, & \text{otherwise} \end{cases}, \tag{158}$$

and

$$\alpha = \frac{1}{\sqrt{K}}. \tag{159}$$

In our setting, using $k_{m=1}$ as input parameter available from the U_{ML} block, we redefine the formula of (152) via a unitary $\tilde{U}_{\text{DSTFT}}^\dagger$, as

$$\tilde{U}_{\text{DSTFT}}^\dagger(|k_m\rangle, h) = \frac{1}{\sqrt{K}} \sum_{j=0}^{K-1} f_W(j-h) e^{-2\pi i j k_1 / K} |j\rangle = |\psi_{k_m}\rangle, \tag{160}$$

where we set $f_W(j-h)$ to unity,

$$f_W(j-h) = 1. \tag{161}$$

Thus, applying (160) on (157) yields

$$\begin{aligned} & \tilde{U}_{\text{DSTFT}}^\dagger \left(\alpha \sum_{m=1}^M \sum_{k_m=1}^{K_m} |k_1 + x_{m,k_m}\rangle \right) \\ &= \frac{1}{\sqrt{K}} \sum_{j=0}^{K-1} \left(\alpha \sum_{m=0}^{M-1} \sum_{k_m=0}^{K_m-1} e^{-2\pi i j k_1 / K} \right) e^{-2\pi i j x_{m,k_m} / K} |j\rangle \\ &= \frac{1}{\sqrt{K}} \left(\sum_{j=0}^{K-1} e^{-2\pi i j x_{m,k_m} / K} \right) \left(\alpha \sum_{m=0}^{M-1} \sum_{k_m=0}^{K_m-1} e^{-2\pi i j k_1 / K} \right) |j\rangle, \end{aligned} \tag{162}$$

where

$$j = \frac{K}{k_m}, \tag{163}$$

and $\sum_{j=0}^{K-1} e^{-2\pi i j x_{m,k_m} / K} = 1$, thus (162) can be rewritten as

$$\begin{aligned} & \tilde{U}_{\text{DSTFT}}^\dagger \left(\alpha \sum_{m=1}^M \sum_{k_m=1}^{K_m} |k_1 + x_{m,k_m}\rangle \right) \\ &= \frac{1}{\sqrt{K}} \left(\alpha \sum_{m=0}^{M-1} \sum_{k_m=0}^{K_m-1} e^{-2\pi i \left(\frac{K}{k_m}\right) k_1 / K} \right) \left| \frac{K}{k_m} \right\rangle. \end{aligned} \tag{164}$$

As follows, if

$$j = \frac{K}{k_1}, \tag{165}$$

then, the resulting $\text{Pr}(j)$ probability is

$$\begin{aligned} \text{Pr}(j) &= \frac{1}{K} \left| \alpha \sum_{k=0}^{K_1-1} e^{-2\pi i j k_1 / K} \right|^2 \\ &= \frac{1}{K} \left| \alpha \sum_{k=0}^{K_1-1} e^{-2\pi i \frac{K}{k_1} k_1 / K} \right|^2 \\ &= \frac{1}{K} |\alpha|^2 K_1^2 \\ &= \frac{1}{K^2} K_1^2, \end{aligned} \tag{166}$$

while for the remaining j -s, the probabilities are vanished out, thus

$$\text{Pr}(j) = 0, \tag{167}$$

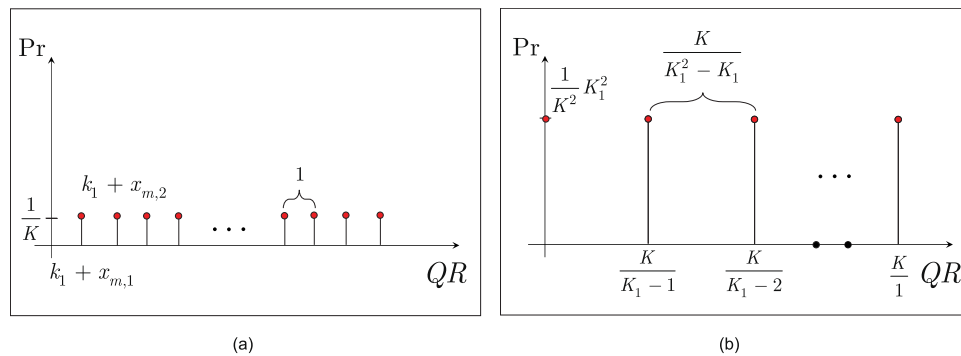


Figure 4. (a) The state of the QR quantum register after the $\tilde{U}_{\text{CQT}}^\dagger$ operation. The quantum register contains $K = \sum_m K_m$ states, $|k_1 + x_{m,k_m}\rangle$, each with probability $|\alpha|^2 = 1/K$, with a unit distance between the states (depicted by the red dots). (b) The state of the QR quantum register after the $\tilde{U}_{\text{DSTFT}}^\dagger$ operation. The quantum register contains K_1 quantum states, $|\frac{K}{k_1}\rangle, k_1 = 0, \dots, K_1 - 1$, each with probability $\frac{1}{K} |\alpha|^2 K_1^2 = \frac{1}{K^2} K_1^2$, with a distance $\frac{K}{K_1 - K_1}$ between the states (depicted by the red dots; the vanished-out states of the quantum register are depicted by the black dots).

if

$$j \neq \frac{K}{k_1}. \tag{168}$$

Therefore, applying the U_{DFT} discrete quantum Fourier transform on the resulting system state (164), defined in our setting as

$$U_{\text{DFT}}(|k\rangle) = \frac{1}{\sqrt{K_1}} \sum_{j=0}^{K_1-1} e^{2\pi ijk/K_1} |j\rangle, \tag{169}$$

yields the source system $m = 1$ in terms of the K_1 bases, as

$$U_{\text{DFT}} \tilde{U}_{\text{DSTFT}}^\dagger \left(\alpha \sum_{m=1}^M \sum_{k_m=1}^{K_m} |k_1 + x_{m,k_m}\rangle \right) = \frac{1}{\sqrt{K_1}} \sum_{k_m=1}^{K_1} |k_1\rangle = |\Phi^*\rangle, \tag{170}$$

that identifies the target system from (35).

The proof is concluded here. ■

The state of the QR quantum register after the $\tilde{U}_{\text{CQT}}^\dagger$ operation and after the $\tilde{U}_{\text{DSTFT}}^\dagger$ operation is depicted in Fig. 4.

Retrieval Efficiency

This section evaluates the retrieval efficiency of an HRE quantum memory in terms of the achievable output SNR values.

Theorem 4. (Retrieval efficiency of an HRE quantum memory). *The SNR of the output quantum system of an HRE quantum memory is evolvable from the difference of the wave function energy ratios taken between the input system, the quantum register system, and the output quantum system.*

Proof. Let $|\psi_{in}\rangle$ be an arbitrary quantum system fed into the input of an HRE quantum memory unit,

$$|\psi_{in}\rangle = \sum_i a_i |i\rangle, \tag{171}$$

and let $|\phi\rangle$ be the state outputted from the QR quantum register,

$$|\phi\rangle = U_{\text{QR}} |\psi_{in}\rangle, \tag{172}$$

where U_{QG} is an unknown transformation.

Let $|\Phi^*\rangle$ be the output system of as given in (170), that can be rewritten as

$$|\Phi^*\rangle = U|\phi\rangle = U(U_{QR}|\psi_{in}\rangle), \quad (173)$$

where U is the operator of the integrated unitary operations of the HRE quantum memory, defined as

$$U = U_{ML}\tilde{U}_{DSTFT}^\dagger U_{DFT} = U_F U_{CQT} U_P U_{CQT}^\dagger \tilde{U}_{DSTFT}^\dagger U_{DFT}. \quad (174)$$

Then, let \mathcal{O}_V be a verification oracle that computes the energy E of a wavefunction $|\psi\rangle = \sum_i c_i |\varphi_i\rangle$ ¹³³ as

$$E(\psi) = \frac{\int \langle \psi | \hat{H} | \psi \rangle}{\int \langle \psi | \psi \rangle} = \frac{\sum_{ij} c_i^* c_j \int \langle \varphi_i | \hat{H} | \varphi_j \rangle}{\sum_{ij} c_i^* c_j \int \langle \varphi_i | \varphi_j \rangle}, \quad (175)$$

where \hat{H} is a Hamiltonian.

Then, let evaluate the corresponding energies of wavefunctions $|\psi_{in}\rangle, |\phi\rangle$ and $|\Phi^*\rangle$ via \mathcal{O}_V , as

$$S = E(\psi_{in}), \quad (176)$$

$$X = E(\phi), \quad (177)$$

and

$$T = E(\Phi^*). \quad (178)$$

Then, let Δ be the difference of the ratios of wavefunction energies, defined as

$$\Delta = R(S, T) - R(S, X) \quad (179)$$

where

$$R(S, T) = \frac{S}{T}, \quad (180)$$

and

$$R(S, X) = \frac{S}{X}. \quad (181)$$

From the quantities of (176)–(178), let $\text{SNR}(|\Phi^*\rangle)$ be the SNR of the output system $|\Phi^*\rangle$, defined as

$$\begin{aligned} \text{SNR}(|\Phi^*\rangle) &= 10 \log_{10} R(S, T) \\ &= \log_{10} \Delta + \frac{1}{10} \text{SNR}(|X\rangle), \end{aligned} \quad (182)$$

where

$$\text{SNR}(|X\rangle) = 10 \log_{10} R(S, X), \quad (183)$$

while Δ is as given in (179).

Therefore, the SNR of the output system can be evolved from the difference of the ratios of the wavefunction energies as

$$\begin{aligned} \text{SNR}(|\Phi^*\rangle) &= 10 \log_{10} R(S, T) \\ &= 10(\log_{10} \Delta + \log_{10} R(S, X)) \\ &= 10(\log_{10}(R(S, T) - R(S, X)) + \log_{10} R(S, X)) \\ &= 10\left(\log_{10} \frac{R(S, T)}{R(S, X)} + \log_{10} R(S, X)\right). \end{aligned} \quad (184)$$

It also can be verified that Δ from (179) can be rewritten as

$$\Delta = 10^{\Delta_{\text{SNR}}/10}, \quad (185)$$

where Δ_{SNR} is an SNR difference, defined as

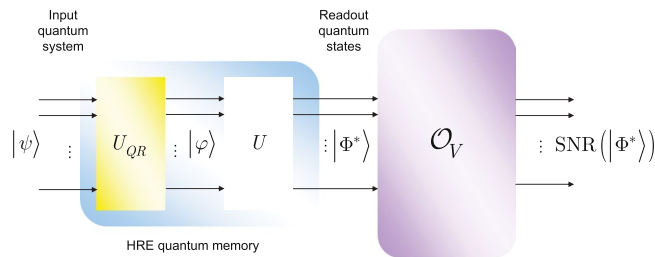


Figure 5. Verification of the retrieval efficiency of an HRE quantum memory unit via an \mathcal{O}_V verification oracle. In the verification procedure, an unknown quantum system $|\psi\rangle$ is stored in the QR quantum register that is evolved by an unknown operation U_{QR} of the QR quantum register. The output of QR is an unknown quantum system $|\phi\rangle$ that is processed further by the U integrated unitary operations of the HRE quantum memory. The output system of the HRE quantum memory is $|\Phi^*\rangle$ (170). The \mathcal{O}_V oracle evaluates the SNR of the readout quantum system $|\Phi^*\rangle$.

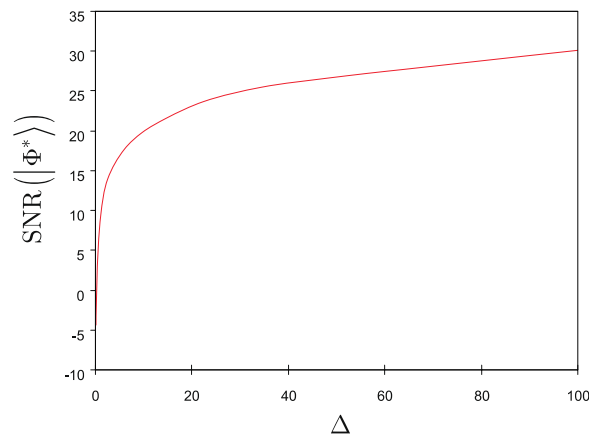


Figure 6. The output SNR values, $\text{SNR}(|\Phi^*\rangle) = 10 \log_{10} R(S, T)$, of an HRE quantum memory in the function of $\Delta = R(S, T) - R(S, X)$, where $R(S, T) = \frac{S}{T}$, $R(S, X) = \frac{S}{X}$, $S = E(\psi_m)$, $X = E(\phi)$, and $T = E(\Phi^*)$.

$$\Delta_{\text{SNR}} = \text{SNR}(|\Phi^*\rangle) - \text{SNR}(|X\rangle). \quad (186)$$

The high SNR values are reachable at moderate values of wavefunction energy ratio differences (179), therefore a high retrieval efficiency (high SNR values) can be produced by the local unitaries of the memory unit (see also Fig. 5).

The proof is concluded here. ■

The verification of the retrieval efficiency of the output of an HRE quantum memory unit is depicted in Fig. 5. The output SNR values in the function of the Δ wave function energy ratio difference are depicted in Fig. 6.

Conclusions

Quantum memories are a cornerstone of the construction of quantum computers and a high-performance global-scale quantum Internet. Here, we defined the HRE quantum memory for near-term quantum devices. We defined the unitary operations of an HRE quantum memory and proved the learning procedure. We showed that the local unitaries of an HRE quantum memory integrates a group of quantum machine learning operations for the evaluation of the unknown quantum system, and a group of unitaries for the target system recovery. We determined the achievable output SNR values. The HRE quantum memory is a particularly convenient unit for gate-model quantum computers and the quantum Internet.

Ethics statement. This work did not involve any active collection of human data.

Data availability

This work does not have any experimental data.

Received: 30 August 2019; Accepted: 12 December 2019;

Published online: 10 January 2020

References

- Pirandola, S. & Braunstein, S. L. Unite to build a quantum internet. *Nature* **532**, 169–171 (2016).
- Lloyd, S. *et al.* Infrastructure for the quantum Internet. *ACM SIGCOMM Computer Communication Review* **34**, 9–20 (2004).
- Pirandola, S. End-to-end capacities of a quantum communication network. *Commun. Phys.* **2**, 51 (2019).
- Wehner, S., Elkouss, D. & Hanson, R. Quantum internet: A vision for the road ahead. *Science* **362**, 6412 (2018).
- Van Meter, R. *Quantum Networking*. ISBN 1118648927, 9781118648926, John Wiley and Sons Ltd (2014).
- Kimble, H. J. The quantum Internet. *Nature* **453**, 1023–1030 (2008).
- Van Meter, R., Ladd, T. D., Munro, W. J. & Nemoto, K. System Design for a Long-Line Quantum Repeater. *IEEE/ACM Transactions on Networking* **17**(3), 1002–1013 (2009).
- Van Meter, R., Satoh, T., Ladd, T. D., Munro, W. J. & Nemoto, K. Path selection for quantum repeater networks. *Networking Science* **3**(1–4), 82–95 (2013).
- Van Meter, R. & Devitt, S. J. Local and Distributed Quantum Computation. *IEEE Computer* **49**(9), 31–42 (2016).
- Pirandola, S., Laurenza, R., Ottaviani, C. & Banchi, L. Fundamental limits of repeaterless quantum communications. *Nature Communications*, **15043**, <https://doi.org/10.1038/ncomms15043> (2017).
- Pirandola, S. *et al.* Theory of channel simulation and bounds for private communication. *Quantum Sci. Technol.* **3**, 035009 (2018).
- Pirandola, S. Capacities of repeater-assisted quantum communications. *Quantum Sci. Technol.* **4**, 045006 (2019).
- Gyongyosi, L. & Imre, S. Decentralized Base-Graph Routing for the Quantum Internet. *Physical Review A*, American Physical Society, <https://doi.org/10.1103/PhysRevA.98.022310> (2018).
- Gyongyosi, L. & Imre, S. Dynamic topology resilience for quantum networks. *Proc. SPIE 10547*, Advances in Photonics of Quantum Computing, Memory, and Communication XI, 105470Z, <https://doi.org/10.1117/12.2288707> (2018).
- Gyongyosi, L. & Imre, S. Topology Adaption for the Quantum Internet. *Quantum Information Processing*. <https://doi.org/10.1007/s11128-018-2064-x> (2018). Springer Nature.
- Gyongyosi, L. & Imre, S. Entanglement Access Control for the Quantum Internet. *Quantum Information Processing*, Springer Nature, <https://doi.org/10.1007/s11128-019-2226-5> (2019).
- Gyongyosi, L. & Imre, S. Opportunistic Entanglement Distribution for the Quantum Internet, *Scientific Reports*, Nature, <https://doi.org/10.1038/s41598-019-38495-w> (2019).
- Gyongyosi, L. & Imre, S. Adaptive Routing for Quantum Memory Failures in the Quantum Internet, *Quantum Information Processing*, Springer Nature, <https://doi.org/10.1007/s11128-018-2153-x> (2018).
- Quantum Internet Research Group (QIRG), web: <https://datatracker.ietf.org/rg/qirg/about/> (2018).
- Laurenza, R. & Pirandola, S. General bounds for sender-receiver capacities in multipoint quantum communications. *Phys. Rev. A* **96**, 032318 (2017).
- Gyongyosi, L. & Imre, S. Multilayer Optimization for the Quantum Internet, *Scientific Reports*, Nature, <https://doi.org/10.1038/s41598-018-30957-x> (2018).
- Gyongyosi, L. & Imre, S. Entanglement Availability Differentiation Service for the Quantum Internet, *Scientific Reports*, Nature, <https://doi.org/10.1038/s41598-018-28801-3>, <https://www.nature.com/articles/s41598-018-28801-3> (2018).
- Gyongyosi, L. & Imre, S. Entanglement-Gradient Routing for Quantum Networks, *Scientific Reports*, Nature, <https://doi.org/10.1038/s41598-017-14394-w>, <https://www.nature.com/articles/s41598-017-14394-w> (2017).
- Gyongyosi, L. & Imre, S. A Survey on Quantum Computing Technology, *Computer Science Review*, Elsevier, <https://doi.org/10.1016/j.cosrev.2018.11.002>, ISSN: 1574-0137 (2018).
- Rozpedek, F. *et al.* Optimizing practical entanglement distillation. *Phys. Rev. A* **97**, 062333 (2018).
- Humphreys, P. *et al.* Deterministic delivery of remote entanglement on a quantum network. *Nature* **558** (2018).
- Liao, S.-K. *et al.* Satellite-to-ground quantum key distribution. *Nature* **549**, 43–47 (2017).
- Ren, J.-G. *et al.* Ground-to-satellite quantum teleportation. *Nature* **549**, 70–73 (2017).
- Hensen, B. *et al.* Loophole-free Bell inequality violation using electron spins separated by 1.3 kilometres. *Nature* **526** (2015).
- Hucul, D. *et al.* Modular entanglement of atomic qubits using photons and phonons. *Nature Physics* **11**(1) (2015).
- Noelleke, C. *et al.* Efficient Teleportation Between Remote Single-Atom Quantum Memories. *Physical Review Letters* **110**, 140403 (2013).
- Sangouard, N. *et al.* Quantum repeaters based on atomic ensembles and linear optics. *Reviews of Modern Physics* **83**, 33 (2011).
- Caleffi, M. End-to-End Entanglement Rate: Toward a Quantum Route Metric, 2017 *IEEE Globecom*, <https://doi.org/10.1109/GLOCOMW.2017.8269080> (2018).
- Caleffi, M. Optimal Routing for Quantum Networks. *IEEE Access* Vol 5, <https://doi.org/10.1109/ACCESS.2017.2763325> (2017).
- Caleffi, M., Cacciapuoti, A. S. & Bianchi, G. Quantum Internet: from Communication to Distributed Computing, *arXiv:1805.04360* (2018).
- Castelvecchi, D. The quantum internet has arrived, *Nature*, News and Comment, <https://www.nature.com/articles/d41586-018-01835-3> (2018).
- Cacciapuoti, A. S. *et al.* Quantum Internet: Networking Challenges in Distributed Quantum Computing, *arXiv:1810.08421* (2018).
- Chakraborty, K., Rozpedeky, F., Dahlbergz, A. & Wehner, S. Distributed Routing in a Quantum Internet, *arXiv:1907.11630v1* (2019).
- Khatiri, S., Matyas, C. T., Siddiqui, A. U. & Dowling, J. P. Practical figures of merit and thresholds for entanglement distribution in quantum networks. *Phys. Rev. Research* **1**, 023032 (2019).
- Kozłowski, W. & Wehner, S. Towards Large-Scale Quantum Networks. *Proc. of the Sixth Annual ACM International Conference on Nanoscale Computing and Communication*, Dublin, Ireland, *arXiv:1909.08396* (2019).
- Pathumsoot, P. *et al.* Modeling of Measurement-based Quantum Network Coding on IBMQ Devices. *arXiv:1910.00815v1* (2019).
- Pal, S., Batra, P., Paterek, T. & Mahesh, T. S. Experimental localisation of quantum entanglement through monitored classical mediator. *arXiv:1909.11030v1* (2019).
- Briegel, H. J., Dur, W., Cirac, J. I. & Zoller, P. Quantum repeaters: the role of imperfect local operations in quantum communication. *Phys. Rev. Lett.* **81**, 5932–5935 (1998).
- Dur, W., Briegel, H. J., Cirac, J. I. & Zoller, P. Quantum repeaters based on entanglement purification. *Phys. Rev. A* **59**, 169–181 (1999).
- Van Loock, P. *et al.* Hybrid quantum repeater using bright coherent light. *Phys. Rev. Lett.* **96**, 240501 (2006).
- Simon, C. *et al.* Quantum Repeater with Photon Pair Sources and Multimode Memories. *Phys. Rev. Lett.* **98**, 190503 (2007).
- Sangouard, N., Dubessy, R. & Simon, C. Quantum repeaters based on single trapped ions. *Phys. Rev. A* **79**, 042340 (2009).
- Gyongyosi, L. & Imre, S. Training Optimization for Gate-Model Quantum Neural Networks, *Scientific Reports*, Nature, <https://doi.org/10.1038/s41598-019-48892-w> (2019).
- Gyongyosi, L. & Imre, S. Dense Quantum Measurement Theory, *Scientific Reports*, Nature, <https://doi.org/10.1038/s41598-019-43250-2> (2019).
- Gyongyosi, L. & Imre, S. State Stabilization for Gate-Model Quantum Computers, *Quantum Information Processing*, Springer Nature, <https://doi.org/10.1007/s11128-019-2397-0> (2019).
- Gyongyosi, L. & Imre, S. Quantum Circuit Design for Objective Function Maximization in Gate-Model Quantum Computers, *Quantum Information Processing*, <https://doi.org/10.1007/s11128-019-2326-2> (2019).
- Preskill, J. Quantum Computing in the NISQ era and beyond. *Quantum* **2**, 79 (2018).

53. Arute, F. *et al.* Quantum supremacy using a programmable superconducting processor. *Nature* **574**, <https://doi.org/10.1038/s41586-019-1666-5> (2019).
54. Harrow, A. W. & Montanaro, A. Quantum Computational Supremacy. *Nature* **549**, 203–209 (2017).
55. Aaronson, S. & Chen, L. Complexity-theoretic foundations of quantum supremacy experiments. *Proceedings of the 32nd Computational Complexity Conference, CCC '17*, pages 22:1–22:67 (2017).
56. Farhi, E., Goldstone, J., Gutmann, S. & Neven, H. Quantum Algorithms for Fixed Qubit Architectures. *arXiv:1703.06199v1* (2017).
57. Farhi, E. & Neven, H. Classification with Quantum Neural Networks on Near Term Processors, *arXiv:1802.06002v1* (2018).
58. Alexeev, Y. *et al.* Quantum Computer Systems for Scientific Discovery, *arXiv:1912.07577* (2019).
59. Loncar, M. *et al.* Development of Quantum InterConnects for Next- Generation Information Technologies, *arXiv:1912.06642* (2019).
60. Lloyd, S. & Weedbrook, C. Quantum generative adversarial learning. *Phys. Rev. Lett.* **121**, arXiv:1804.09139 (2018).
61. Gisin, N. & Thew, R. Quantum Communication. *Nature Photon* **1**, 165–171 (2007).
62. Xiao, Y. F. & Gong, Q. Optical microcavity: from fundamental physics to functional photonics devices. *Science Bulletin* **61**, 185–186 (2016).
63. Zhang, W. *et al.* Quantum Secure Direct Communication with Quantum Memory. *Phys. Rev. Lett.* **118**, 220501 (2017).
64. Enk, S. J., Cirac, J. I. & Zoller, P. Photonic channels for quantum communication. *Science* **279**, 205–208 (1998).
65. Duan, L. M., Lukin, M. D., Cirac, J. I. & Zoller, P. Long-distance quantum communication with atomic ensembles and linear optics. *Nature* **414**, 413–418 (2001).
66. Zhao, B., Chen, Z. B., Chen, Y. A., Schmiedmayer, J. & Pan, J. W. Robust creation of entanglement between remote memory qubits. *Phys. Rev. Lett.* **98**, 240502 (2007).
67. Goebel, A. M. *et al.* Multistage Entanglement Swapping. *Phys. Rev. Lett.* **101**, 080403 (2008).
68. Tittel, W. *et al.* Photon-echo quantum memory in solid state systems. *Laser Photon. Rev* **4**, 244–267 (2009).
69. Dur, W. & Briegel, H. J. Entanglement purification and quantum error correction. *Rep. Prog. Phys* **70**, 1381–1424 (2007).
70. Sheng, Y. B. & Zhou, L. Distributed secure quantum machine learning. *Science Bulletin* **62**, 1025–1029 (2017).
71. Leung, D., Oppenheim, J. & Winter, A. *IEEE Trans. Inf. Theory* **56**, 3478–90. (2010).
72. Kobayashi, H., Le Gall, F., Nishimura, H. & Rotteler, M. Perfect quantum network communication protocol based on classical network coding. *Proceedings of 2010 IEEE International Symposium on Information Theory (ISIT)* pp 2686–90 (2010).
73. Petz, D. *Quantum Information Theory and Quantum Statistics 6* (Springer-Verlag, Heidelberg, Hiv, 2008).
74. Lloyd, S. Capacity of the noisy quantum channel. *Physical Rev. A* **55**, 1613–1622 (1997).
75. Lloyd, S. The Universe as Quantum Computer. *A Computable Universe: Understanding and exploring Nature as computation*, Zenil, H. ed., World Scientific, Singapore, *arXiv:1312.4455v1* (2013).
76. Shor, P. W. Scheme for reducing decoherence in quantum computer memory. *Phys. Rev. A* **52**, R2493–R2496 (1995).
77. Chou, C. *et al.* Functional quantum nodes for entanglement distribution over scalable quantum networks. *Science* **316**(5829), 1316–1320 (2007).
78. Muralidharan, S., Kim, J., Lutkenhaus, N., Lukin, M. D. & Jiang, L. Ultrafast and Fault-Tolerant Quantum Communication across Long Distances. *Phys. Rev. Lett.* **112**, 250501 (2014).
79. Yuan, Z. *et al.* *Nature* **454**, 1098–1101 (2008).
80. Kobayashi, H., Le Gall, F., Nishimura, H. & Rotteler, M. General scheme for perfect quantum network coding with free classical communication. *Lecture Notes in Computer Science* (Automata, Languages and Programming SE-52 vol. 5555), Springer) pp 622–633 (2009).
81. Hayashi, M. Prior entanglement between senders enables perfect quantum network coding with modification. *Physical Review A* **76**, 040301(R) (2007).
82. Hayashi, M., Iwama, K., Nishimura, H., Raymond, R. & Yamashita, S. Quantum network coding. *Lecture Notes in Computer Science* (STACS 2007 SE52 vol. 4393) ed. Thomas, W. & Weil, P. (Berlin Heidelberg: Springer) (2007).
83. Chen, L. & Hayashi, M. Multicopy and stochastic transformation of multipartite pure states. *Physical Review A* **83**(2), 022331 (2011).
84. Schoute, E., Mancinska, L., Islam, T., Kerenidis, I. & Wehner, S. Shortcuts to quantum network routing. *arXiv:1610.05238* (2016).
85. Distante, E. *et al.* Storing single photons emitted by a quantum memory on a highly excited Rydberg state. *Nat. Commun.* **8**, 14072, <https://doi.org/10.1038/ncomms14072> (2017).
86. Albrecht, B., Farrera, P., Heinze, G., Cristiani, M. & de Riedmatten, H. Controlled rephasing of single collective spin excitations in a cold atomic quantum memory. *Phys. Rev. Lett.* **115**, 160501 (2015).
87. Choi, K. S. *et al.* Mapping photonic entanglement into and out of a quantum memory. *Nature* **452**, 67–71 (2008).
88. Chaneliere, T. *et al.* Storage and retrieval of single photons transmitted between remote quantum memories. *Nature* **438**, 833–836 (2005).
89. Fleischhauer, M. & Lukin, M. D. Quantum memory for photons: Dark-state polaritons. *Phys. Rev. A* **65**, 022314 (2002).
90. Korber, M. *et al.* Decoherence-protected memory for a single-photon qubit. *Nature Photonics* **12**, 18–21 (2018).
91. Yang, J. *et al.* Coherence preservation of a single neutral atom qubit transferred between magic-intensity optical traps. *Phys. Rev. Lett.* **117**, 123201 (2016).
92. Ruster, T. *et al.* A long-lived Zeeman trapped-ion qubit. *Appl. Phys. B* **112**, 254 (2016).
93. Neuzner, A. *et al.* Interference and dynamics of light from a distance-controlled atom pair in an optical cavity. *Nat. Photon* **10**, 303–306 (2016).
94. Yang, S.-J., Wang, X.-J., Bao, X.-H. & Pan, J.-W. An efficient quantum light-matter interface with sub-second lifetime. *Nat. Photon.* **10**, 381–384 (2016).
95. Uphoff, M., Brekenfeld, M., Rempe, G. & Ritter, S. An integrated quantum repeater at telecom wavelength with single atoms in optical fiber cavities. *Appl. Phys. B* **122**, 46 (2016).
96. Zhong, M. *et al.* Optically addressable nuclear spins in a solid with a six-hour coherence time. *Nature* **517**, 177–180 (2015).
97. Sprague, M. R. *et al.* Broadband single-photon-level memory in a hollow-core photonic crystal fibre. *Nat. Photon* **8**, 287–291 (2014).
98. Gouraud, B., Maxein, D., Nicolas, A., Morin, O. & Laurat, J. Demonstration of a memory for tightly guided light in an optical nanofiber. *Phys. Rev. Lett.* **114**, 180503 (2015).
99. Razavi, M., Piani, M. & Lutkenhaus, N. Quantum repeaters with imperfect memories: Cost and scalability. *Phys. Rev. A* **80**, 032301 (2009).
100. Langer, C. *et al.* Long-lived qubit memory using atomic ions. *Phys. Rev. Lett.* **95**, 060502 (2005).
101. Maurer, P. C. *et al.* Room-temperature quantum bit memory exceeding one second. *Science* **336**, 1283–1286 (2012).
102. Steger, M. *et al.* Quantum information storage for over 180 s using donor spins in a 28Si semiconductor vacuum. *Science* **336**, 1280–1283 (2012).
103. Bar-Gill, N., Pham, L. M., Jarmola, A., Budker, D. & Walsworth, R. L. Solid-state electronic spin coherence time approaching one second. *Nature Commun* **4**, 1743 (2013).
104. Riedl, S. *et al.* Bose-Einstein condensate as a quantum memory for a photonic polarisation qubit. *Phys. Rev. A* **85**, 022318 (2012).
105. Xu, Z. *et al.* Long lifetime and high-fidelity quantum memory of photonic polarisation qubit by lifting Zeeman degeneracy. *Phys. Rev. Lett.* **111**, 240503 (2013).
106. Zhu, F., Zhang, W., Sheng, Y. B. & Huang, Y. D. Experimental long-distance quantum secret direct communication. *Sci. Bull* **62**, 1519 (2017).

107. Wu, F. Z. *et al.* High-capacity quantum secure direct communication with two-photon six-qubit hyperentangled states. *Sci. China Phys. Mech. Astron.* **60**, 120313 (2017).
108. Chen, S. S., Zhou, L., Zhong, W. & Sheng, Y. B. Three-step three-party quantum secure direct communication. *Sci. China Phys. Mech. Astron.* **61**, 090312 (2018).
109. Niu, P. H. *et al.* Measurement-device-independent quantum communication without encryption. *Sci. Bull.* **63**, 1345–1350 (2018).
110. Biamonte, J. *et al.* Quantum Machine Learning. *Nature* **549**, 195–202 (2017).
111. Lloyd, S., Mohseni, M. & Rebentrost, P. Quantum algorithms for supervised and unsupervised machine learning. *arXiv:1307.0411* (2013).
112. Lloyd, S., Mohseni, M. & Rebentrost, P. Quantum principal component analysis. *Nature Physics* **10**, 631 (2014).
113. Kok, P. *et al.* Linear optical quantum computing with photonic qubits. *Rev. Mod. Phys.* **79**, 135–174 (2007).
114. Bacsardi, L. On the Way to Quantum-Based Satellite Communication. *IEEE Comm. Mag.* **51**(08), 50–55 (2013).
115. Gyongyosi, L., Imre, S. & Nguyen, H. V. A Survey on Quantum Channel Capacities. *IEEE Communications Surveys and Tutorials*, <https://doi.org/10.1109/COMST.2017.2786748> (2018).
116. Gyongyosi, L., Bacsardi, L. & Imre, S. A Survey on Quantum Key Distribution, *Infocom. J XI*, 2, pp. 14–21 (2019).
117. Imre, S. & Gyongyosi, L. *Advanced Quantum Communications - An Engineering Approach*. (Wiley-IIEEE Press, New Jersey, 2013).
118. Chien, J.-T. *Source Separation and Machine Learning*. Academic Press (2019).
119. Yang, P.-K., Hsu, C.-C. & Chien, J.-T., Bayesian factorization and selection for speech and music separation. In: *Proc. of Annual Conference of International Speech Communication Association*, pp. 998–1002 (2014).
120. Yang, P.-K., Hsu, C.-C. & Chien, J.-T., Bayesian singing-voice separation. In: *Proc. of Annual Conference of International Society for Music Information Retrieval (ISMIR)*, pp. 507–512 (2014).
121. Chien, J.-T. & Yang, P.-K. Bayesian factorization and learning for monaural source separation. *IEEE/ACM Transactions on Audio, Speech and Language Processing* **24**(1), 185–195 (2016).
122. Bishop, C. M. *Pattern Recognition and Machine Learning*. Springer Science (2006).
123. Vembu, S. & Baumann, S. Separation of vocals from polyphonic audio recordings. In: *Proc. of ISMIR*, pages 375–378 (2005).
124. Lee, D. D. & Seung, H. S. Algorithms for nonnegative matrix factorization. *Advances in Neural Information Processing Systems*, 556–562 (2000).
125. Cemgil, A. T. Bayesian inference for nonnegative matrix factorisation models. *Computational Intelligence and Neuroscience*, 785152 (2009).
126. Schmidt, M. N., Winther, O. & Hansen, L. K. Bayesian non-negative matrix factorization. In: *Proc. of ICA*, 540–547 (2009).
127. Tibshirani, R. Regression shrinkage and selection via the lasso. *Journal of the Royal Statistical Society. Series B* **58**(1), 267–288 (1996).
128. Brown, J. C. Calculation of a Constant Q spectral transform. *Journal of the Acoustic Society of America* **89**(1), 425–434 (1991).
129. Quatieri, T. F. *Discrete-Time Speech Signal Processing: Principles and Practice*, Prentice Hall, ISBN-10: 013242942X, ISBN-13: 978-0132429429 (2002).
130. Jaiswal, R. *et al.* Clustering NMF Basis Functions Using Shifted NMF for Monaural Sound Source Separation. *IEEE International Conference on Acoustics, Speech and Signal Processing (ICASSP)* (2011).
131. FitzGerald, D., Cranitch, M. & Coyle, E. Shifted Nonnegative matrix factorisation for sound source separation. *IEEE Workshop of Statistical Signal Processing*, Bordeaux, France (2005).
132. Bader, B. W. & Kolda, T. G. MATLAB Tensor Classes for Fast Algorithm Prototyping, Sandia National Laboratories Report, SAND2004-5187 (2004).
133. Sherrill, C. D. A Brief Review of Elementary Quantum Chemistry, Lecture Notes, web: <http://vergil.chemistry.gatech.edu/notes/quantrev/quantrev.html> (2001).

Acknowledgements

The research reported in this paper has been supported by the National Research, Development and Innovation Fund (TUDFO/51757/2019-ITM, Thematic Excellence Program). This work was partially supported by the National Research Development and Innovation Office of Hungary (Project No. 2017-1.2.1-NKP-2017-00001), by the Hungarian Scientific Research Fund - OTKA K-112125 and in part by the BME Artificial Intelligence FIKP grant of EMMI (BME FIKP-MI/SC).

Author contributions

L.G.Y. designed the protocol and wrote the manuscript. L.G.Y. and S.I. analyzed the results. All authors reviewed the manuscript.

Competing interests

The authors declare no competing interests.

Additional information

Supplementary information is available for this paper at <https://doi.org/10.1038/s41598-019-56689-0>.

Correspondence and requests for materials should be addressed to L.G.Y.

Reprints and permissions information is available at www.nature.com/reprints.

Publisher's note Springer Nature remains neutral with regard to jurisdictional claims in published maps and institutional affiliations.



Open Access This article is licensed under a Creative Commons Attribution 4.0 International License, which permits use, sharing, adaptation, distribution and reproduction in any medium or format, as long as you give appropriate credit to the original author(s) and the source, provide a link to the Creative Commons license, and indicate if changes were made. The images or other third party material in this article are included in the article's Creative Commons license, unless indicated otherwise in a credit line to the material. If material is not included in the article's Creative Commons license and your intended use is not permitted by statutory regulation or exceeds the permitted use, you will need to obtain permission directly from the copyright holder. To view a copy of this license, visit <http://creativecommons.org/licenses/by/4.0/>.

© The Author(s) 2020